



**Politecnico  
di Torino**

**Politecnico di Torino**

Master of Science in Civil Engineering  
Y.Y. 2024/2025  
December 2025

# **Study on Hydraulic and Hydrological Invariance**

Analysis and Assessment Across Different Regions of Italy

**Advisors:**

Prof. BUTERA Ilaria  
Prof. BOANO Fulvio  
Prof. GANORA Daniele

**Author:**

Ana Maria Azcarate Garcia  
ID: 321233



# Acknowledgments

I would like to express my sincere gratitude to my thesis supervisors for their guidance, patience and steady support throughout this work. Their expertise and thoughtful feedback helped shape the direction of the research and strengthened its overall quality.

I am also grateful to the professors of the Hydrology and Hydraulic Engineering group at Politecnico di Torino. Their courses, insights and dedication provided the foundations on which this thesis was built, and they contributed greatly to my development as an engineer.

My appreciation also goes to Politecnico di Torino as an institution. The environment of curiosity, research and academic rigor that it fosters has played an important role in my growth during these years, and I am thankful for the opportunities and resources that made this journey possible.

I am grateful to my family for their constant support and encouragement.

I am equally grateful to my friends, whose understanding, motivation and companionship have accompanied me throughout this process. They made the difficult days lighter and the achievements even more meaningful.

Finally, I thank God and my cat Copito for giving me the strength, clarity and perseverance needed to complete this work.

To all of you, thank you.

# Abstract

Urbanization alters the natural hydrological balance by increasing impervious surfaces, which reduces infiltration and amplifies peak runoff. To address these impacts, several Italian regional regulations introduced the concept of hydraulic and hydrologic invariance, ensuring that post-development runoff conditions remain comparable to pre-development ones. This study aimed to evaluate how the application of a single regulatory framework—the Lombardy Regional Regulation (R.R. 19 April 2019, n. 8)—affects the design of detention volumes when applied to different climatic contexts across Italy. The research focused on understanding how variations in rainfall characteristics influence the sizing of stormwater detention systems under a uniform set of design criteria, in order to assess the robustness and adaptability of the regulation beyond its regional scope.

The research was based on a reference case study representing a typical commercial area composed of a shopping center, parking areas, and a green zone. Six cities were selected according to the Köppen climate classification and rainfall data from the FOCA database, covering a wide range of climatic conditions. The methodology followed the hydrological procedure prescribed by the regulation, applying the most critical parameters at each step to represent the most conservative design scenario.

The results showed that, despite the large variability in rainfall intensity and distribution among the selected cities, the calculated detention volumes differed across locations but ultimately remained below the minimum regulatory threshold. As a result, all designs were governed by the minimum storage requirement established by the Lombardy Regulation, leading to a single, uniform solution consisting of a detention structure for temporary storage (and also the possible integration of infiltration systems or other innovative sustainable approaches) and controlled discharge to the sewer network. This outcome highlights that the normative thresholds tend to dominate over local climatic variability, ensuring hydraulic safety under all tested scenarios but potentially leading to over-dimensioned solutions in regions with lower rainfall intensity.

**Keywords:** hydraulic invariance, stormwater management, Lombardy Regulation, detention basin, urban drainage.



# Contents

Introduction . . . . .	9
<b>1 Problem Statement and Methods</b>	<b>11</b>
1.1 Description of the Problem and Importance . . . . .	11
1.2 Urbanization and Loss of Pervious Surfaces . . . . .	12
1.3 Hydraulic and Hydrologic Invariance . . . . .	13
1.4 Regulatory Framework:Lombardy Regional Regulation (R.R. 19 April 2019, No. 8) . . . . .	14
1.4.1 Overview of the Regulation . . . . .	14
1.4.2 Calculation Procedure According to the Regulation . .	15
<b>2 Case Study and Investigated Areas</b>	<b>33</b>
2.1 Criteria for City Selection and Data Sources . . . . .	33
2.2 Selected Cities, Rainfall Conditions, and Groundwater Levels .	37
2.2.1 Selected Cities . . . . .	37
2.2.2 Rainfall Data . . . . .	38
2.2.3 Groundwater Levels . . . . .	39
2.3 Construction Site and Characteristics . . . . .	40
2.3.1 Surface Types and Land Use . . . . .	40
2.3.2 Surface Materials . . . . .	42
2.3.3 Slopes and Drainage Patterns . . . . .	44
2.3.4 Drainage System Details . . . . .	45
<b>3 Results and Discussion</b>	<b>47</b>
3.1 Calculation of the Design Storage Volume According to the Lombardy Regulation . . . . .	47
3.2 Stormwater Detention System Design . . . . .	60
3.2.1 Proposed SuDS Solution Based on Modular Geocellu- lar Structures . . . . .	60
3.2.2 Hydraulic Design . . . . .	63
3.3 Design Drawings . . . . .	74
3.4 Discussion of Results . . . . .	84
3.4.1 Comparison Between Hydrological Volumes and the Normative Minimum . . . . .	84
3.4.2 Overall Interpretation . . . . .	85
<b>Conclusions</b> . . . . .	<b>86</b>
<b>References</b>	<b>88</b>

# List of Figures

1.1	Conceptual comparison between natural and urbanized catchments showing reduced infiltration and increased surface runoff	13
1.2	<i>Cartographic representation of areas with different levels of hydraulic criticality, from Annex B [1]</i>	17
1.3	Horton's law — Infiltration capacity trend under conditions of water abundance on the pervious surface (from Annex F) [1]	23
1.4	Horton curve parameters proposed by the [7]	24
1.5	Identification using the rainfall-only method of the critical event $D_W$ and the corresponding critical storage volume $W_0$ , that is, the one that maximizes the stored volume[1]	26
1.6	Representation of the storage (lamination) process from Annex G [1]	29
1.7	Optimal lamination with equal stored volume $W$ (above) and with equal maximum outflow discharge $Q_{u,max}$ (below), from Annex G[1]	29
2.1	Köppen climate classification map of Italy used for the preliminary selection of representative climatic regions [8]	33
2.2	Legend of the Köppen climate classification used in the Italian climatic analysis [8]	34
2.3	FOCA raster dataset showing the spatial distribution of rainfall intensity parameters across Italy [17]	35
2.4	Geographical location of the six selected Italian cities considered in the hydraulic invariance analysis: Torino, Genova, Aosta, Roma, Cagliari and Palermo	37
2.5	Overview of the case study (Google Earth Pro) [24]	41
2.6	Parking lot surface	42
2.7	Sidewalk surface	43
2.8	Green areas	43
2.9	Green areas.	44
2.10	Green areas	44
2.11	stormwater inlet identified along the mall boundary	45
2.12	Collector channel located inside the parking lot	46
3.1	Exemplary Scheme No. 6 of the interventions to which the hydraulic and hydrologic invariance measures must be applied, from Annex A [1]	47

3.2	Table A of the Regional Regulation of Lombardy (R.R. Lombardia) 19 April 2019 [1] . . . . .	48
3.3	Chicago hyetograph with a duration of 30 minutes and a return period of 50 years, for the city of Aosta . . . . .	50
3.4	Chicago hyetograph with a duration of 30 minutes and a return period of 50 years, for the city of Cagliari . . . . .	51
3.5	Chicago hyetograph with a duration of 30 minutes and a return period of 50 years, for the city of Palermo . . . . .	51
3.6	Chicago hyetograph with a duration of 30 minutes and a return period of 50 years, for the city of Torino . . . . .	52
3.7	Chicago hyetograph with a duration of 30 minutes and a return period of 50 years, for the city of Roma . . . . .	52
3.8	Chicago hyetograph with a duration of 30 minutes and a return period of 50 years, for the city of Genova . . . . .	53
3.9	Comparison of the 30-minute design Chicago hyetographs ( $T = 50$ years, $r = 0.4$ ) for the six study sites. The different peak intensities highlight the spatial variability of short-duration rainfall across Italy. . . . .	53
3.10	<i>Sub-basins scheme</i> . . . . .	54
3.11	Inflow Hydrograph – Aosta . . . . .	55
3.12	Inflow Hydrograph – Cagliari . . . . .	56
3.13	Inflow Hydrograph – Palermo . . . . .	56
3.14	Inflow Hydrograph – Torino . . . . .	57
3.15	Inflow Hydrograph – Roma . . . . .	57
3.16	Inflow Hydrograph – Genova . . . . .	58
3.17	Proposed retention/lamination area schemes in LID systems [1] . . . . .	61
3.18	Examples of surface laminating structures consisting of open-air basins and channels [1] . . . . .	61
3.19	Examples of surface laminating structures consisting of open-air basins and channels [1] . . . . .	62
3.20	Example of a geocellular SuDS detention system during a storm event, showing temporary subsurface water storage. Image courtesy of [27]. . . . .	62
3.21	Installation phase of a geocellular modular system for subsurface stormwater detention. The modular units provide high storage capacity and structural strength. Image courtesy of [27]. . . . .	63
3.22	Geocellular modular unit selected for the subsurface storage system (dimensions: $680 \times 410 \times 450$ mm). Image source: Greening Solution [32] . . . . .	71

3.23	General plan view of the study area, showing the layout of the surface drainage elements, the location of the detention basins and subsurface tanks, and the direction of stormwater flow across the site. Scale 1:1000 . . . . .	75
3.24	Plan view of the FIRST-FLUSH TANK and Detention Basin 1. Scale 1:250 [33]. . . . .	76
3.25	Plan view of the FIRST-FLUSH TANK and Detention Basin 2. Scale 1:250 [33]. . . . .	77
3.26	Section view of the detention basin 1 and subsurface tank, showing the surface basin geometry, the stratigraphy of the soil and granular layers, and the connection to the underlying geocellular storage system scale 1:50[33]. . . . .	78
3.27	Section view of the detention basin 2 and subsurface tank, showing the surface basin geometry, the stratigraphy of the soil and granular layers, and the connection to the underlying geocellular storage system. scale 1:50 [33]. . . . .	79
3.28	Longitudinal section of the detention basin and subsurface tank, showing the natural ground level (NGL), the geocellular storage system, and the technical compartment housing the submersible electric pump ( $Q = 10 \text{ L/s}$ ) and its discharge connection to the public stormwater network. scale 1:50 . . . .	80
3.29	3D model of the proposed stormwater detention system – View 1 - Close-up view [34] . . . . .	81
3.30	3D model of the proposed stormwater detention system – View 2 - Detention basin displayed in its dry (empty) condition [34]	82
3.31	3D model of the proposed stormwater detention system – View 3 - Detention basin shown at its maximum water level [34] . .	83
3.32	Comparison between minimum required volume ( $V_{\min}$ ) and design detention volume ( $V_{\det}$ ) for the six cities. . . . .	85

# List of Tables

1.1	<i>Table showing the calculation method from [1]</i> . . . . .	18
2.1	Representative Köppen climate types, associated cities, precipitation ranges, and data sources. . . . .	34
2.2	FOCA-based rainfall intensity (I) and depth (D) values for candidate cities [17] . . . . .	36
2.3	List of selected cities. . . . .	37
2.4	Design depth values for Duration = 15 min (mm) and for different return periods obtained using the GEV distribution .	38
2.5	Design depth values for Duration = 15 min (mm) and for different return periods obtained using the Gumbel distribution	38
2.6	Design intensity values for Duration=15 min (mm/h) and for different return periods obtained using the GEV distribution .	39
2.7	Design intensity values for Duration=15 min (mm/h) and for different return periods obtained using the Gumbel distribution	39
2.8	Groundwater levels for the six selected cities, based on official hydrogeological sources. . . . .	40
2.9	<i>Surface types and land use – construction site</i> . . . . .	41
2.10	<i>Surface types and materials – construction site</i> . . . . .	42
3.1	Parameters of the rainfall curves for each city . . . . .	50
3.2	Peak inflow discharge obtained for each study city . . . . .	58
3.3	Detention volumes obtained for each study city . . . . .	59

# Introduction

Urban development modifies the natural hydrological cycle by expanding impervious surfaces and reducing the ability of the soil to infiltrate stormwater. These changes increase runoff generation and intensify peak discharges, placing significant pressure on drainage infrastructures and heightening the risk of urban flooding. In response to these challenges, several Italian regions have adopted regulatory frameworks aimed at maintaining hydraulic and hydrologic invariance, ensuring that post-development runoff conditions do not exceed the natural behaviour of the catchment.

Among these frameworks, the Lombardy Regional Regulation (R.R. 19 April 2019, n. 8) stands out for its high level of procedural detail and methodological clarity. Its structured guidelines for rainfall characterisation, runoff estimation and detention-volume calculation make it a robust reference for analyses that require consistency and comparability.

The central problem addressed in this thesis concerns how a single development scenario responds when placed in different climatic contexts across Italy while being evaluated under one uniform regulatory framework. Holding all methodological and normative assumptions constant allows the study to isolate the effect of climate and to determine the detention volumes obtained for each city. In this way, the research explores how storage requirements vary across distinct rainfall regimes and how climatic differences influence the hydrological behaviour of the same case study.

The reference project consists of a typical commercial development composed of paved areas, a shopping centre and surrounding green spaces—an urban configuration commonly encountered in contemporary land-use planning. Six Italian cities were selected to represent a wide spectrum of climatic conditions, ranging from alpine to Mediterranean environments. For each location, the hydrological analysis follows strictly the procedure prescribed by the Lombardy Regulation, without introducing local adjustments, thereby ensuring a fully homogeneous basis for comparison.

Beyond quantifying the variation in detention volumes, the thesis also examines the possible stormwater management solutions that may be adopted to ensure compliance with the regulation in each scenario. This involves considering the suitability of different design approaches and understanding how regulatory constraints influence their implementation in diverse environmental contexts.

By adopting a uniform methodological approach across multiple climatic settings, this thesis contributes to a deeper understanding of the interaction between regulatory criteria, climatic variability and stormwater design. The findings support broader reflections on the applicability of region-specific

regulations outside their original context, and on the relevance of design criteria that are capable of adapting to varied hydrological environments.

# Chapter 1

## Problem Statement and Methods

### 1.1 Description of the Problem and Importance

Urbanization and the consequent alteration of the natural hydrological cycle have made stormwater management one of the main challenges in contemporary land planning. In this context, many regional authorities in Italy have introduced regulatory frameworks aimed at mitigating the hydrological impact of new developments by requiring that post-development runoff does not exceed pre-development conditions. Among them, the Regolamento Regionale Lombardia 19 aprile 2019, n. 8 [1] provides one of the most structured and quantitative approaches to the concept of hydraulic and hydrologic invariance.

The present study investigates the applicability and effectiveness of this Lombardy regulation when applied to urban contexts characterized by different climatic conditions across Italy. The analysis is conducted by considering a single reference case study, representing a typical commercial area composed of a shopping center, parking lots, and a green zone. By maintaining identical land-use characteristics and surface distribution for all test sites, the only varying factors among the selected cities are the local climatic conditions and precipitation regimes. Since the objective is to evaluate the regulation under diverse environmental conditions, the analysis consistently adopts the most critical design parameters for each location, ensuring that the comparison reflects a conservative and technically robust approach. This choice allows the assessment of how the required detention volume and related design parameters vary across climatic zones when subject to the same regulatory constraints. The core problem lies in understanding how a regulation conceived for a specific regional context—Lombardy—behaves when extended to territories with diverse rainfall patterns, soil permeability, and hydrological behavior. The analysis aims to assess whether the same regulatory prescriptions lead to consistent and technically sustainable results in terms of detention volumes and design parameters, and to quantify how the required storage volume varies among different climatic zones.

By applying a uniform regulatory framework to multiple case studies, the research seeks to identify potential discrepancies and sensitivities related to climatic variability. This comparative approach provides insight into the robustness of the current regulatory method and its possible limitations when



transferred to regions with markedly different hydrological behavior.

Ultimately, this work contributes to a better understanding of how local climatic factors influence the design outcomes imposed by hydraulic and hydrologic invariance principles. The findings are expected to support future discussions on the adaptability of regional regulations and the need for more flexible, climate-sensitive design criteria in urban stormwater management.

## 1.2 Urbanization and Loss of Pervious Surfaces

Urbanization profoundly modifies the hydrological balance of natural catchments. The transformation of pervious land into impervious surfaces—such as roads, parking lots, and rooftops—reduces infiltration and storage capacity, leading to an increase in both the volume and peak rate of surface runoff. As a result, rainfall that would naturally infiltrate or be temporarily retained on the ground is rapidly conveyed into the drainage network, causing higher flow concentrations and potentially overloading existing infrastructures.

As highlighted by [2], infiltration is the key process controlling the partition of rainfall into surface runoff and subsurface flow, and its alteration directly affects groundwater recharge and water quality. Consequently, the reduction of pervious surfaces in urban areas not only compromises the natural infiltration process but also amplifies the risks of flooding and degradation of receiving water bodies.

These alterations not only affect the hydraulic performance of stormwater systems but also generate environmental and water quality issues. Increased runoff often carries sediments, hydrocarbons, and other urban pollutants, contributing to the degradation of receiving water bodies. Moreover, the reduction of infiltration compromises groundwater recharge, altering the long-term hydrological equilibrium of the basin.

From a design perspective, this change in the hydrological response of urban areas necessitates the adoption of control measures capable of mitigating the excess runoff and restoring conditions comparable to the pre-development state. For this reason, regional and national authorities have progressively adopted policies and technical criteria aimed at preserving or re-establishing the original hydrologic behavior of the territory. The hydraulic and hydrologic invariance principle emerges from this context as a planning tool to ensure that the impact of urbanization on the local water cycle remains within sustainable limits (further discussed in Section 1.3).

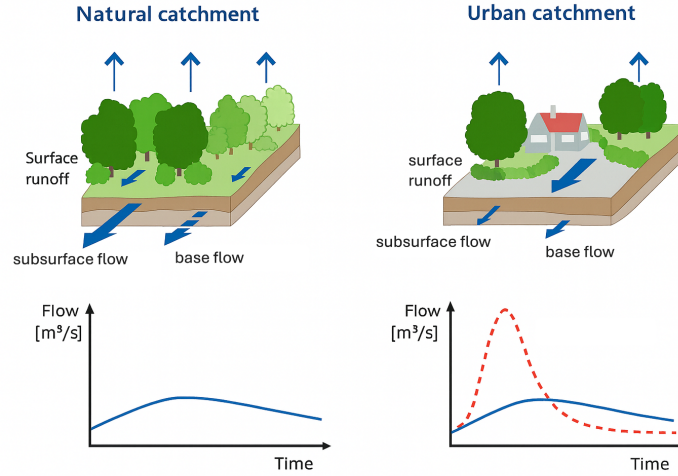


**Figure 1.1:** *Conceptual comparison between natural and urbanized catchments showing reduced infiltration and increased surface runoff*

### 1.3 Hydraulic and Hydrologic Invariance

The concept of hydraulic and hydrologic invariance represents one of the most relevant approaches in modern stormwater management and sustainable land planning. It is based on the principle that any new development must not worsen the hydraulic and hydrological conditions of the site compared to its pre-development state. In practice, this means ensuring that the quantity and peak rate of runoff discharged into the drainage system after construction remain comparable to those existing before the intervention [2] , [3].

Hydraulic invariance focuses on maintaining the same peak discharge by introducing storage or flow regulation systems that compensate for the increased imperviousness of urban surfaces. On the other hand, hydrologic invariance extends this concept by considering the entire water balance of the site, aiming to preserve not only the peak flow but also the total runoff volume and the processes of infiltration and evapotranspiration that contribute to groundwater recharge [2].

To achieve these conditions, various control measures are adopted, ranging from structural interventions—such as detention basins, infiltration trenches, permeable pavements, and green roofs—to non-structural planning tools that limit the extent of impervious surfaces [4]. The design and sizing of these facilities are typically regulated by regional or national standards, which define the criteria for acceptable post-development discharge rates and storage capacities. Among these, the [1] provides one of the most structured and

quantitative frameworks for implementing the invariance principle.

The practical relevance of this principle can be interpreted through the fundamental mechanisms described in hydrological theory: as discussed by [3], the increase in surface runoff and peak discharge is a direct consequence of altered rainfall–runoff dynamics, while the reduction of infiltration affects the subsurface and groundwater components of the water balance [2]. These processes justify the need for design criteria capable of restoring pre-development flow conditions through detention and infiltration measures.

Further details on the specific application of the Lombardy regulation are provided in Section 1.4.

## 1.4 Regulatory Framework: Lombardy Regional Regulation (R.R. 19 April 2019, No. 8)

### 1.4.1 Overview of the Regulation

The *Regional Regulation of Lombardy* (R.R. 19 April 2019, n. 8) [1], which updates and integrates the previous R.R. 23 November 2017, n. 7, defines the technical and procedural criteria for ensuring *hydraulic and hydrologic invariance* in urban and territorial transformations. This regulation was issued in accordance with *Article 58-bis* of the *Regional Law n. 12/2005 – Law for the Government of the Territory*, with the objective of progressively restoring the natural hydrological regime, mitigating the hydraulic risk linked to urbanization, and promoting sustainable territorial development.

The main principle established by the regulation is that post-development runoff conditions must not exceed the pre-development discharge regime, in order to preserve the hydrological balance of the territory. To achieve this goal, the regulation promotes the design and implementation of local stormwater management measures that collect, store, infiltrate, and reuse rainwater directly at the source. These include infiltration systems, detention and retention basins, permeable pavements, green roofs, and other nature-based solutions that allow the reduction and temporal redistribution of stormwater volumes.

In addition to the general provisions, the regulation includes a set of Annexes (A–M), which contain schematic examples, technical guidelines, calculation procedures, and design parameters necessary for the practical implementation of the invariance principle:

- Annex A illustrates exemplary schemes of the types of interventions to which the hydraulic and hydrologic invariance criteria must be applied.

- Annex B provides the list of hydrographic basins and sub-basins characterized by different levels of hydraulic criticality, identifying areas at high, medium, and low hydraulic risk.
- Annex C lists the municipalities that fall within each of these criticality categories, specifying their classification as “Area A”, “Area B”, or “Area C”. This classification determines the design parameters to be adopted—such as the maximum allowable discharge ( $Q_{lim}$ ) and the minimum storage volume per hectare ( $V_{min}$ )—as established in Article 7 and the related tables.
- Annex F and Annex G define the methodologies for calculating *infiltration processes* and *storage (detention) volumes*, respectively, providing the necessary formulas, parameters, and boundary conditions.
- Annex H presents practical examples that illustrate the application of the calculation methodologies introduced in Annexes F and G.
- Annex I describes typical configurations for outlet structures connecting detention basins to receiving water bodies.
- Annex L contains *technical construction guidelines and examples of best practices* for sustainable urban drainage (SUDS), including green roofs, infiltration trenches, vegetated swales, and permeable pavements.
- Annex M defines the procedure for *monetary compensation (monetizzazione)*, which allows the financial offsetting of the required measures when direct on-site implementation of hydraulic invariance is not technically feasible.

Overall, the Lombardy Regulation provides a quantitative, site-specific, and sustainability-oriented framework for stormwater management, harmonizing hydraulic safety requirements with environmental protection and long-term territorial resilience.

## 1.4.2 Calculation Procedure According to the Regulation

### Identification of the Applicable Case (Annex A)

In the first phase, as required by [1], the *Annex A* is consulted to identify which of the exemplary intervention schemes best represents the type of project under consideration. This annex provides schematic examples of

various categories of land-use transformations to which the hydraulic and hydrologic invariance criteria must be applied, or conversely, where they are not required. Through this classification, it is possible to determine whether the specific project is subject to the application of the invariance principle and to select the most representative intervention scheme.

### **Classification of the project area**

In order to account for the different effects that the inflow of additional stormwater may produce on both urban and extra-urban drainage systems, the Regulation [1] divides the regional territory according to the *level of hydraulic criticality* of the receiving watercourse basins. The subdivision is defined as follows:

- *Area A* – high hydraulic criticality: areas that include the territories of the municipalities listed in Annex C, located—either entirely or partially—within the hydrographic basins indicated in Annex B;
- *Area B* – medium hydraulic criticality: areas that include the territories of the municipalities listed in Annex C, not included in Area A and located—either entirely or partially—within reclamation and irrigation districts;
- *Area C* – low hydraulic criticality: areas that include the territories of the municipalities listed in Annex C, not included in Areas A or B.

To determine the classification of the municipality in which the planned transformation will take place, *Annex B – List of hydrographic basins or portions of basins with high hydraulic criticality and mapping of areas with different levels of criticality* provides a map of the Lombardy Region showing the criticality zones (Figure 1.2) and the hydrographic basins with high hydraulic criticality.

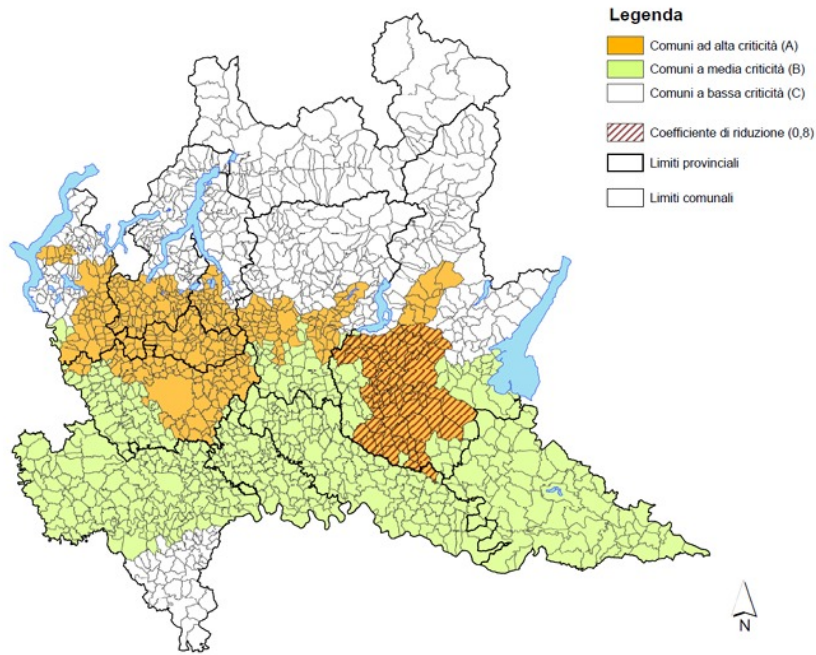


**Figure 1.2:** *Cartographic representation of areas with different levels of hydraulic criticality, from Annex B [1]*

Based on the area of hydraulic criticality, the Regional Regulation defines the admissible values of stormwater discharge ( $u_{lim}$ ) into the receiving systems, as listed below:

- for *Area A*: 10 l/s per hectare of impervious draining surface of the intervention;
- for *Area B*: 20 l/s per hectare of impervious draining surface of the intervention;
- for *Area C*: 20 l/s per hectare of impervious draining surface of the intervention.

The discharges into the receiving bodies coming from combined sewer overflow systems or from public stormwater drainage networks, related to the draining surfaces located in Areas A and B that are already urbanized and equipped with sewer systems, must be limited through appropriate measures so that the outflow remains within values compatible with the hydraulic capacity of the receptor, and in any case not exceeding the maximum admissible value of 40 l/s per hectare of impervious surface.

It should be noted that the manager of the receiving systems, in cases of limited hydraulic capacity, may impose more restrictive discharge limits where necessary.

### Determination of the Intervention Class

Once the hydraulic criticality area in which the project is located has been identified, the *class of intervention* to which the urban transformation belongs is determined according to Table 1.1. This classification depends on:

- the surface area, which refers to the lot affected by the intervention and not to the entire development zone;
- the weighted average runoff coefficient, defined as:

$$\varphi_m = \frac{\sum_i A_i \varphi_i}{\sum_i A_i} \quad (1.1)$$

where  $A_i$  represents the surface area and  $\varphi_i$  the runoff coefficient of the  $i$ -th sub-catchment.

The Regulation specifies that the soil permeability to be considered for the calculation must correspond to the pre-existing conditions prior to urbanization.

CLASSE DI INTERVENTO		SUPERFICIE INTERESSATA DALL'INTERVENTO	COEFFICIENTE DEFLUSSO MEDIO PONDERALE	MODALITÀ DI CALCOLO	
				AMBITI TERRITORIALI	
				(articolo 7)	
				Aree A, B	Aree C
0	Impermeabilizzazione potenziale qualsiasi	≤ 0,03 ha (≤ 300 mq)	qualsiasi	Requisiti minimi articolo 12 comma 1	
1	Impermeabilizzazione potenziale bassa	da > 0,03 a ≤ 0,1 ha (da > 300 mq a ≤ 1.000 mq)	≤ 0,4	Requisiti minimi articolo 12 comma 2	
2	Impermeabilizzazione potenziale media	da > 0,03 a ≤ 0,1 ha (da > 300 a ≤ 1.000 mq)	> 0,4	Metodo delle sole piogge (vedi articolo 11 e allegato G)	Requisiti minimi articolo 12 comma 2
		da > 0,1 a ≤ 1 ha (da > 1.000 a ≤ 10.000 mq)	qualsiasi		
		da > 1 a ≤ 10 ha (da > 10.000 a ≤ 100.000 mq)	≤ 0,4		
3	Impermeabilizzazione potenziale alta	da > 1 a ≤ 10 ha (da > 10.000 a ≤ 100.000 mq)	> 0,4	Procedura dettagliata (vedi articolo 11 e allegato G)	
		> 10 ha (> 100.000 mq)	qualsiasi		

**Table 1.1:** Table showing the calculation method from [1]

For interventions with medium or high potential impermeabilization (Classes 2 and 3), the project shall include:

- analysis of design rainfall and inflow hydrographs;

- estimation of infiltration capacity in soils and infiltration structures;
- computation of detention storage and emptying time;
- verification of outlet discharges to ensure compliance with the admissible limits ( $Q_{\text{lim}}$ );
- detailed design of collection, conveyance, detention, infiltration, and discharge works.

For interventions with low potential impermeabilization (Class 1), a simplified procedure may be adopted, while for small interventions ( $S \leq 300 \text{ m}^2$ ) no full hydraulic invariance project is required.

The design must be developed following the methodologies of Annexes F and G, using the reference return periods established by the Regulation:

- $T = 50$  years for the design of storage and infiltration structures;
- $T = 100$  years for safety verification.

Overall, the regulation requires that the hydraulic and hydrologic design be proportional to the complexity and scale of the intervention, ensuring technical feasibility and compliance with the principles of stormwater invariance.

### **Project precipitation calculation**

For both methods, the calculation proceeds with the estimation of the design rainfall. The Regulation [1] refers to the characteristic parameters of the *rainfall probability curves* provided by ARPA Lombardia, while allowing the use of alternative datasets only when more specific or updated official data are available for the site of interest, provided that their source and validity are properly documented.

The parameters of the curve are expressed in the following form:

$$h = a_1 w_T D^n$$

$$w_T = \varepsilon + \frac{\alpha}{k} \left[ 1 - \left( \ln \left( \frac{T}{T-1} \right) \right)^k \right]$$

where  $h$  is the rainfall depth,  $D$  the duration, and  $a$  the pluviometric coefficient.  $w_T$  is the probabilistic factor associated with the return period  $T$ ,  $n$  is the exponent of the curve, and  $\alpha$ ,  $\varepsilon$ , and  $k$  are the parameters of the adopted GEV (Generalized Extreme Value) probability distribution.



### Brief recall the most typical distributions: Gumbel and GEV

The methodology of L-moments is briefly recalled here; for more details, the reader can refer to [5] and [6]. L-moments are based on order statistics, meaning that the sample must be arranged in ascending order so that the generic record of observations is rewritten as  $x_{(1)}, x_{(2)}, \dots, x_{(n)}$ , where  $x_{(i)}$  is the  $i$ -th value of the sorted sample.

The method requires the computation of intermediate variables known as *probability weighted moments* (PWM).

$$\beta_0 = n^{-1} \sum_{i=1}^n x_{i:n} \quad (1.2)$$

$$\beta_1 = n^{-1} \sum_{i=1}^n \frac{(i-1)}{(n-1)} x_{i:n} \quad (1.3)$$

$$\beta_2 = n^{-1} \sum_{i=1}^n \frac{(i-1)(i-2)}{(n-1)(n-2)} x_{i:n} \quad (1.4)$$

$$\beta_r = n^{-1} \sum_{i=1}^n \frac{(i-1)(i-2) \dots (i-r)}{(n-1)(n-2) \dots (n-r)} x_{i:n} \quad (1.5)$$

L-moments are then obtained as linear combinations of PWMs.

$$\lambda_1 = \beta_0 \quad (1.6)$$

$$\lambda_2 = 2\beta_1 - \beta_0 \quad (1.7)$$

$$\lambda_3 = 6\beta_2 - 6\beta_1 + \beta_0 \quad (1.8)$$

$$\lambda_4 = 20\beta_3 - 30\beta_2 + 12\beta_1 - \beta_0 \quad (1.9)$$

The latter are, respectively, a measure of position (L-moment of order 1), dispersion (L-moment of order 2), skewness (L-moment of order 3) and kurtosis (L-moment of order 4) of the sample. It can be noted that the L-moment of order 1 is actually equal to the mean value, that is also the moment of order 1. Further properties of L-moments can be found in [5]. For convenience, dimensionless L-moments ratios are frequently used:

$$\tau \text{ or L-CV} = \frac{\lambda_2}{\lambda_1} \quad (1.10)$$

$$\tau_3 \text{ or L-skewness} = \frac{\lambda_3}{\lambda_2} \quad (1.11)$$

$$\tau_4 \text{ or L-kurtosis} = \frac{\lambda_4}{\lambda_2} \quad (1.12)$$

Sample L-moments can be easily computed from the sample using the equations above and used to calculate the parameters of the Gumbel distribution or its generalization, the generalized extreme value (GEV) distribution. According to [5], the density function of GEV distribution can be written as

$$f(x) = \alpha^{-1} e^{-(1-k)y - e^{-y}}$$

and the cumulative frequency function

$$F(x) = e^{-e^{-y}}$$

with

$$y = \begin{cases} -k^{-1} \log[1 - k(x - \xi)/\alpha] & \text{if } k \neq 0 \\ (x - \xi)/\alpha & \text{if } k = 0 \end{cases}$$

where  $x$  is the variable and  $\xi$ ,  $\alpha$  and  $k$  the location, scale and shape parameters respectively. The case  $k = 0$  corresponds to the Gumbel distribution (note that, with respect to the approach described in the previous section, the Gumbel distribution has parameters named in a different way.) The calculation of the design value can be done by inverting the cumulative frequency function to obtain the quantile function

$$x(F) = \begin{cases} \xi + \alpha[1 - (-\log F)^k]/k & \text{if } k \neq 0 \\ \xi - \alpha \log(-\log F) & \text{if } k = 0 \end{cases}$$

where  $F$  is the non-exceedance frequency, which is related to the return period  $T$  with the well-known expression  $T = 1/(1 - F)$ .

The parameters  $\xi$ ,  $\alpha$  and  $k$  can be estimated with the method of L-moments by means of the following equations, where Hosking and Wallis [5] proposed an approximated functions for  $k$ , as no explicit solution exists:

$$k \approx 7.8590 c + 2.9554 c^2 \quad \text{with} \quad c = \frac{2}{3 + \tau_3} - \frac{\log 2}{\log 3}$$

$$\alpha = \frac{\lambda_2 k}{(1 - 2^{-k}) \Gamma(1 - k)}$$

$$\xi = \lambda_1 - \alpha[1 - \Gamma(1 + k)]/k$$

being  $\Gamma$  the Gamma function. In the case of the Gumbel distribution ( $k = 0$ ), the parameters read

$$\alpha = \frac{\lambda_2}{\log 2}$$

$$\xi = \lambda_1 - \gamma\alpha$$

being  $\gamma$  the Euler's constant equal to approximately 0.5772.

Once the sample L-moments have been calculated, they are used to estimate the parameters of the selected probability distribution, typically the Gumbel or the Generalized Extreme Value (GEV) distribution. These parameters allow deriving the rainfall depth or intensity associated with different return periods by means of the corresponding quantile function. In practice, for each chosen return period  $T$  (e.g., 10, 20, 50, 100 years), the design rainfall  $h_T$  is obtained from the fitted distribution, enabling the construction of the IDF (Intensity–Duration–Frequency) relationships used in the subsequent hydrologic analysis.

### **Methods for calculating infiltration processes**

Subsequently, the evaluation of hydrogeological losses is carried out for the calculation of the net flood hydrograph entering the detention structure. To determine the net hydrograph, it is possible to proceed either by calculating the infiltration process or by adopting a simplified method.

Regarding the first case, infiltration is defined as the flow rate per unit area that, at a given time  $t$ , infiltrates into the subsoil, measured in mm/h. The infiltration model suggested by the Regulation [1] is based on Horton-type models, which describe the infiltration rate as an exponentially decreasing function over time. This model expresses a law that decreases from an initial maximum value  $f_0$ , which depends on the soil type and its initial moisture content at the beginning of the event, to an asymptotic minimum value  $f_c$ , corresponding to the saturated hydraulic conductivity  $K_s$ . The latter depends on the porosity characteristics of the soil, the stratigraphy of the subsoil, and the presence and depth of the groundwater table. The exponential decay is governed by the parameter  $k$ , which defines how rapidly the infiltration rate tends toward the asymptotic value, also related to the soil type.

In design calculations of stormwater control structures, to remain on the conservative side, it is recommended to refer to the minimum asymptotic infiltration value  $f_c$ , which represents the residual infiltration rate once the soil has become substantially saturated. The more an intense rainfall event occurs after previous precipitation, the lower the infiltration capacity due to the partial saturation already reached by the soil.

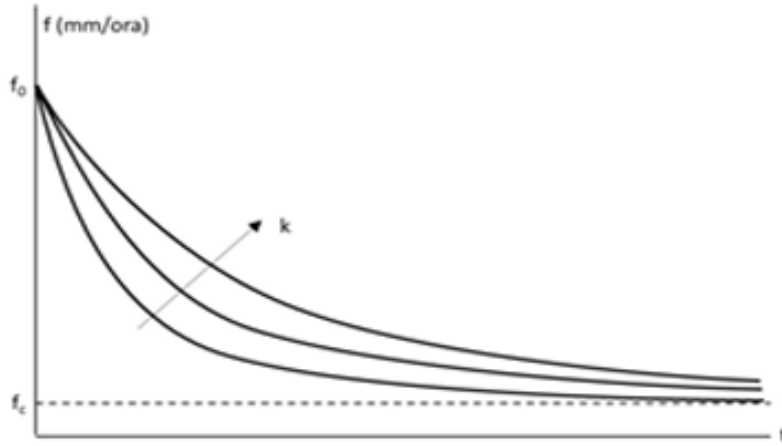


**Figure 1.3:** *Horton's law — Infiltration capacity trend under conditions of water abundance on the pervious surface (from Annex F) [1]*

Regarding the values to be assigned to the parameters of the Horton law, the Soil Conservation Service (SCS) [7], now known as the Natural Resources Conservation Service, proposes the following four classes (A, B, C, D) of soils with grass cover:

- Class A – Low runoff potential: includes deep sands with very little silt and clay; also deep gravelly soils, highly permeable.
- Class B – Moderately low runoff potential: includes the majority of sandy soils that are less deep than those in group A, but that overall maintain high infiltration capacities even at saturation.
- Class C – Moderately high runoff potential: includes fine-textured soils and soils containing significant amounts of clay and colloids, although less than in group D; this group has low infiltration capacity when saturated.
- Class D – High runoff potential: includes most clays with high swelling capacity, as well as thin soils with nearly impermeable horizons close to the surface.

<i>Classe suolo</i>	$f_o$ [mm/ora]	$f_c$ [mm/ora]	$k$ [ore-1]
A	250	25.4	2
B	200	12.7	2
C	125	6.3	2
D	76	2.5	2

**Figure 1.4:** *Horton curve parameters proposed by the [7]*

It is also important to specify that, for the calculation of the infiltration process, the regulation does not allow the possibility of infiltrating stormwater runoff when the groundwater table is close to the ground surface. However, the depth of the groundwater table is not the only discriminant: infiltration must also be excluded depending on the quality of stormwater, the stability of slopes, or possible interference with building foundations or underground levels of existing structures.

#### **calculation of the net hydrograph**

In cases where sufficient data are not available to proceed with the infiltration method described above, the evaluation of hydrological losses for the calculation of the net inflow hydrograph can be carried out in a simplified way, using the following values:

- equal to 1.0 for all sub-areas corresponding to roofs, coverings, and continuous pavements such as streets, driveways, and parking lots;
- equal to 0.7 for green roofs, rooftop gardens, and green areas built on slabs; also for areas intended for water infiltration management according to the present regulation, and for discontinuous permeable pavements such as porous streets, driveways, and parking lots;
- equal to 0.3 for permeable sub-areas of any type, including green areas equipped with water collection and conveyance systems, excluding uncultivated surfaces and agricultural-use areas from the computation.

#### **calculation of the storage volume for stormwater detention**

Once the net hydrograph has been determined, either through the calculation of the infiltration process or by using standardized values, the next step consists in applying the rainfall-only method or the detailed procedure.

#### **Simplified “rainfall-only” method.**

In the case of an intervention belonging to *class 2*, it is necessary to apply the *rainfall-only method*, which is based on the assumption that the inflow hydrograph generated by rainfall,  $Q_e(t)$ , entering the detention basin is a

rectangular hydrograph with duration  $D$  and constant discharge  $Q_e$ . This inflow discharge is equal to the product of the mean rainfall intensity, derived from the IDF curve, and the impermeable drainage area of the intervention contributing to the basin.

In this way, it is assumed that, given the limited extension of the drainage basin, the effect of the rainfall–runoff transformation within the basin and in the drainage network leading to the basin can be neglected. Consequently, the inflow hydrograph entering the basin coincides with the rainfall hyetograph over the impermeable surface of the contributing area. The constant inflow discharge is therefore expressed as:

$$Q_e = S \cdot \varphi \cdot a \cdot D^{n-1}$$

and the total rainfall volume entering the basin is given by:

$$W_e = S \cdot \varphi \cdot a \cdot D^n$$

where  $S$  is the total contributing drainage area to the basin,  $\varphi$  is the weighted average runoff coefficient of the basin,  $D$  is the rainfall duration, and  $a$  and  $n$  are the parameters of the IDF curve. The term  $a = a_i w_T$  depends on the rainfall intensity derived from the probability distribution.

The outflow hydrograph  $Q_{u,\text{lim}}(t)$  is also assumed to be a rectangular hydrograph characterized by a constant discharge  $Q_{u,\text{lim}}$  (optimal lamination), which is set equal to the maximum allowable discharge according to the regulation. It can thus be expressed as:

$$Q_{u,\text{lim}} = S \cdot \varphi \cdot u_{\text{lim}}$$

The total outflow volume during the rainfall event of duration  $D$  is given by:

$$W_u = S \cdot \varphi \cdot u_{\text{lim}} \cdot D$$

where  $u_{\text{lim}}$  is the specific maximum allowable discharge at the outlet.

Based on these simplifying assumptions, the storage volume required for flow attenuation is represented, for each rainfall duration considered, by the difference between the inflow and outflow volumes calculated at the end of the rainfall duration. In this way, the design storage volume corresponds to the *critical event duration*, that is, the rainfall duration producing the maximum storage requirement. Therefore, the maximum volume  $\Delta W$  that must be stored within the detention basin at the end of a rainfall event of generic duration  $D$  is expressed as:

$$\Delta W = W_e - W_u$$

If the maximum condition is expressed mathematically, by differentiating the expression of  $\Delta W$  with respect to the rainfall duration  $D$ , the *critical duration*  $D_w$  for the detention basin can be obtained, and consequently the corresponding storage volume  $W_0$  is derived as follows:

$$D_w = \left( \frac{Q_{u,\text{lim}}}{S \cdot \varphi \cdot a \cdot n} \right)^{\frac{1}{n-1}}$$

$$W_0 = S \cdot \varphi \cdot a \cdot D_w^n - Q_{u,\text{max}} \cdot D_w$$

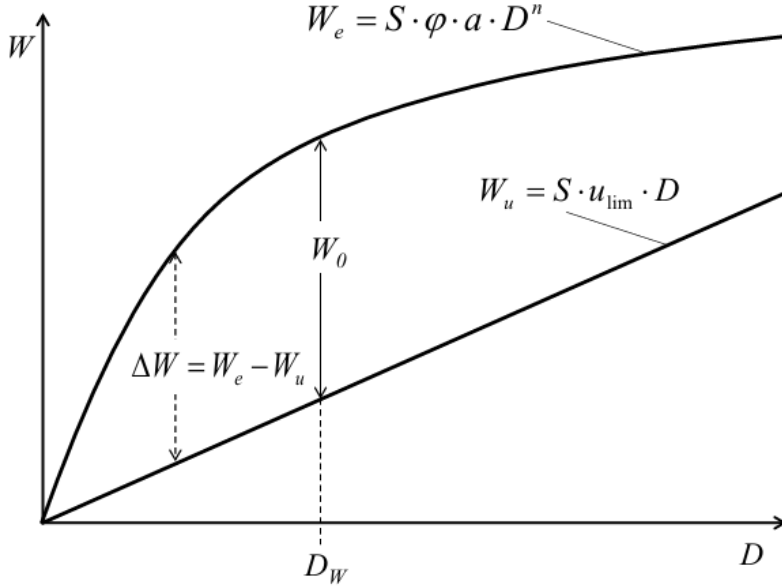


**Figure 1.5:** Identification using the rainfall-only method of the critical event  $D_w$  and the corresponding critical storage volume  $W_0$ , that is, the one that maximizes the stored volume[1]

### Detailed procedure

In the case of a *class 3* intervention, the Regulation requires the adoption of the *detailed procedure*. Therefore, the rainfall-runoff transformation of the basin up to the inlet section of the planned detention basin must be computed in detail. The selection criteria to be adopted are the following:

- *Design hyetograph and total duration* derived from the IDF curve valid for the project area; the use of a Chicago-type design hyetograph is suggested, with a duration greater than the concentration time of the basin draining to the detention structure.

- *Computation of the net hyetograph* based on hydrologic losses due to initial abstractions and infiltration, in relation to soil type and the urbanization planned in the project area.
- *Runoff transformation model* suitable to represent both the formation of the unit hydrographs in the different sub-areas and their propagation, leading to the formation of the overall hydrograph  $Q_e(t)$  at the inlet section of the detention basin; the use of the *time-area method* (“metodo di corrivazione”) of the basin is suggested.

The *Chicago-type hyetograph*, which is also recommended for its relation to the parameters of the GEV probabilistic law previously used for rainfall analysis, is characterized by a peak of maximum intensity and an average intensity for each duration equal to that obtained from the rainfall probability curve. Its construction can be carried out by assigning a duration  $D$  and determining the rainfall depth from the Depth-Duration-Frequency (DDF) curve, expressed in the form:

$$h = a \cdot D^n$$

Considering that the peak may occur at an instant  $t_r = rD$ , with  $r$  ranging between 0 and 1, it is customary to set  $r = 0.4$ , which, in the absence of specific local information, represents an average value derived from studies reported in the literature. Thus, the hyetograph is defined by two equations, one referring to the ascending branch before the peak and the other to the descending branch after the peak:

$$i(t) = n \cdot a \cdot \left( \frac{t_r - t}{r} \right)^{n-1} \quad \text{for } t \leq t_r$$

$$i(t) = n \cdot a \cdot \left( \frac{t - t_r}{1 - r} \right)^{n-1} \quad \text{for } t \geq t_r$$

When selecting the duration of the design hyetograph, it is important to use a duration greater than the concentration time of the catchment area. The distinctive feature of this type of hyetograph is that its shape is not very sensitive to variations in duration: as the duration increases, the area around the peak remains almost unchanged, while the extreme parts of the graph extend. Consequently, hyetographs of longer durations include events with lower probabilities, allowing the assumption that all sub-catchments are contributing simultaneously to the runoff. The design of the detention basin is then carried out by applying the following equations in order to compute the



outflow hydrograph  $Q_u(t)$  from the basin outlet structure, and thus verify compliance with the maximum allowable discharge and the maximum emptying time. The storage and release process over time can be mathematically described by the following system of equations:

- *Continuity equation:*

$$Q_e(t) - Q_u(t) = \frac{dW(t)}{dt}$$

- *Outflow law* governing the outlet/emptying structures:

$$Q_u = Q_u[H(t)]$$

- *Storage curve*, expressing the geometric relationship between the stored volume and the water head in the basin:

$$W = W[H(t)]$$

where  $Q_e(t)$  represents the inflow discharge,  $Q_u(t)$  the total outflow discharge from the outlet, infiltration, and/or reuse systems,  $W(t)$  the stored volume, and  $H(t)$  the water level within the basin. Integrating this system of equations allows the calculation of the three unknown functions  $Q_u(t)$ ,  $H(t)$ , and  $W(t)$ , making it possible to determine their respective maximum values while ensuring that they satisfy the assigned constraints.

When the inflow and outflow hydrographs of a generic basin are plotted, the maximum stored volume  $W_{max}$  corresponds to the area enclosed between the two curves up to the point where the outflow reaches its maximum discharge  $Q_{u,max}$  (see Figure 1.6).

It can be observed that the effect of the detention process consists in a reduction of the peak outflow discharge  $Q_{u,max}$  compared to the peak inflow discharge  $Q_{e,max}$ , as well as in a temporal lag between the two peaks, producing an overall attenuation of the outflow hydrograph compared to the inflow hydrograph.

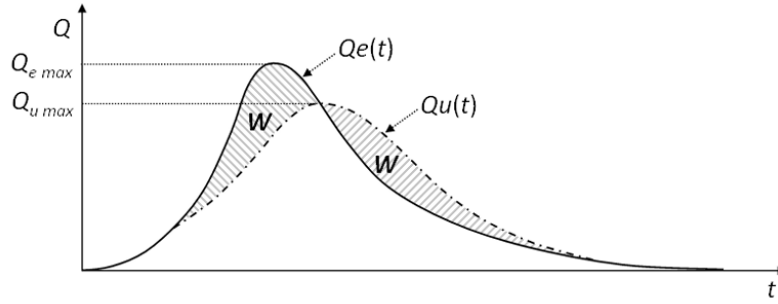


**Figure 1.6:** Representation of the storage (lamination) process from Annex G [1]

In particular, the simplified case of *optimal lamination* is significant, defined as the condition in which the outflow rate remains constant during the peak phase (Figure 1.7). It can be observed that, if the value of  $Q_{u,max}$  is fixed and the outflow rate is kept constantly equal to it, the required storage volume  $W_0$  is minimized. In other words, for a given available storage volume  $W_0$ , the corresponding value of  $Q_{u,max}$  is minimized, thus achieving the maximum lamination effect.

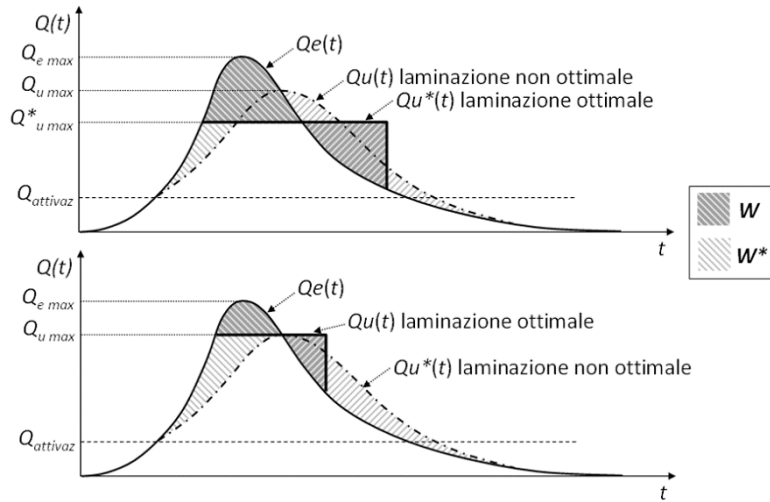


**Figure 1.7:** Optimal lamination with equal stored volume  $W$  (above) and with equal maximum outflow discharge  $Q_{u,max}$  (below), from Annex G[1]

### Calculation of the emptying time

Once the volume to be managed has been determined, the Regional Regulation [1] establishes a limit value for the emptying time of the detention

basins, set at 48 hours, in order to account for the possibility of closely spaced rainfall events. This time is calculated as a function of the outflow and infiltration rates, starting from the maximum stored volume, and is therefore expressed as:

$$t_{svuot} = \frac{W_{lam}}{Q_u + Q_{inf}} \quad (1.13)$$

### Design of the terminal discharge system

The hydraulic structure responsible for regulating and discharging the stormwater flow to the receiving body must consist of a double-chamber inspection manhole, or an equivalent system, allowing full accessibility and measurement of both the discharged flow and the connecting pipes. In any case, the discharge system of the stormwater management works designed to ensure hydraulic and hydrologic invariance must be arranged autonomously with respect to any existing drainage outlet, allowing independent control.

Possible configurations, either by gravity or by pumping systems, connecting the outlet of the detention basin to the receiving body are described in Annex I [1]. For gravity discharges, the diameter of the connecting pipe between the detention basin and the inspection chamber must be determined according to the maximum admissible flow rate at the outlet. Since this diameter could be relatively small, the potential risk of blockage must be considered in the maintenance plan, following Article 13 [1], which prescribes:

1. Periodic inspection of the connecting pipe and other related structures, with frequency increasing as the pipe diameter decreases;
2. Evaluation of the risk of partial or total obstruction during or after a rainfall event, which could prevent the emptying of the basin. In such a case, the responsibility to ensure basin emptying within the time limits indicated in Article 11, paragraph 2(f), remains with the system operator;

Gravity discharge systems must also be equipped with devices preventing the possible surcharge or overflow of the receiving body, which could otherwise cause backflow into the drainage network or into infiltration and detention systems, compromising hydraulic and hydrologic invariance.

Both gravity and pumped discharge systems must be designed to avoid any malfunction or delay in emptying the detention basin, which could lead to extended emptying times and, consequently, to partial filling of the basin during a subsequent rainfall event, thereby reducing the available storage volume required.

### **Minimum requirements for hydraulic and hydrologic invariance measures**

This section of the Regulation [1] defines the minimum design criteria that must be adopted to ensure hydraulic and hydrologic invariance in urban drainage projects. The fundamental objective is to guarantee that post-development runoff does not exceed pre-development conditions, both in terms of peak flow and total discharged volume.

For small interventions involving areas up to 300 m<sup>2</sup>, it is sufficient to provide local infiltration of stormwater into the soil or shallow subsurface layers, without the need for a full hydraulic invariance project. When this is not feasible, the installation of small-scale retention systems can satisfy the minimum regulatory requirement.

For larger interventions or in areas with higher hydraulic criticality, the Regulation requires the construction of detention or storage basins designed to temporarily retain stormwater and release it gradually at a controlled rate. The minimum storage volume of these detention structures depends on the hydraulic criticality of the area:

- 800 m<sup>3</sup> per hectare of impervious drainage area of the intervention, *multiplied by the coefficient  $P'$  indicated in the table reported in Annex C* [1], for areas classified as A with high hydraulic criticality;
- 500 m<sup>3</sup>/ha per hectare of impervious drainage area of the intervention, for areas of medium hydraulic criticality;
- 400 m<sup>3</sup>/ha per hectare of impervious drainage area of the intervention, for areas of low hydraulic criticality.

The discharge from the detention basin into the downstream drainage network or receiving body must always respect the maximum admissible outflow limits established by the Regulation. In the case of gravity discharge, the outlet pipe diameter is determined so that the outflow never exceeds the prescribed limit under full conditions. When this results in a very small diameter, a pumping system may be adopted instead to maintain the required flow control.

Finally, the discharge system must be designed to be fully inspectable and easily maintainable, allowing the measurement and control of both the outflow and infiltration rates, ensuring proper operation of the overall stormwater management system.

### **Maintenance plan for hydraulic and hydrologic invariance systems**

A maintenance plan must be prepared to ensure the long-term efficiency of all systems designed to guarantee hydraulic and hydrologic invariance. The level of detail of the plan must correspond to the complexity of the implemented drainage infrastructure.

The plan should include a complete inventory and the technical characteristics of all structures forming part of the stormwater drainage system, such as infiltration basins, detention tanks, conduits, channels, inspection chambers, and terminal discharge systems.

It must also define both the description and periodicity of the maintenance operations, distinguishing between ordinary and extraordinary interventions. These activities are aimed at maintaining or restoring the hydraulic efficiency of the system and must cover the following components:

- rainwater inlets, gutters, and collection points;
- conduits, pipes, and channels conveying stormwater to the terminal discharge point;
- infiltration systems and subsurface drainage networks;
- detention basins and their control or safety devices;
- any pumping systems discharging to the receiving body;
- the connecting pipeline between the detention structure and the final outlet.

Regular inspection and maintenance of these elements are essential to ensure the correct functioning of the system, prevent clogging or degradation, and preserve the designed storage and discharge capacities over time.

# Chapter 2

## Case Study and Investigated Areas

### 2.1 Criteria for City Selection and Data Sources

The selection of the study cities was carried out through a two-step procedure. The first step consisted of analysing the Köppen climate classification of Italy and the mean annual precipitation associated with each climatic region. Using the Köppen map (Figure 2.1), the different climatic zones present within the Italian territory were identified. For each climate type, representative cities were examined together with their corresponding average annual precipitation values obtained from official sources such as ARPA and regional environmental agencies.

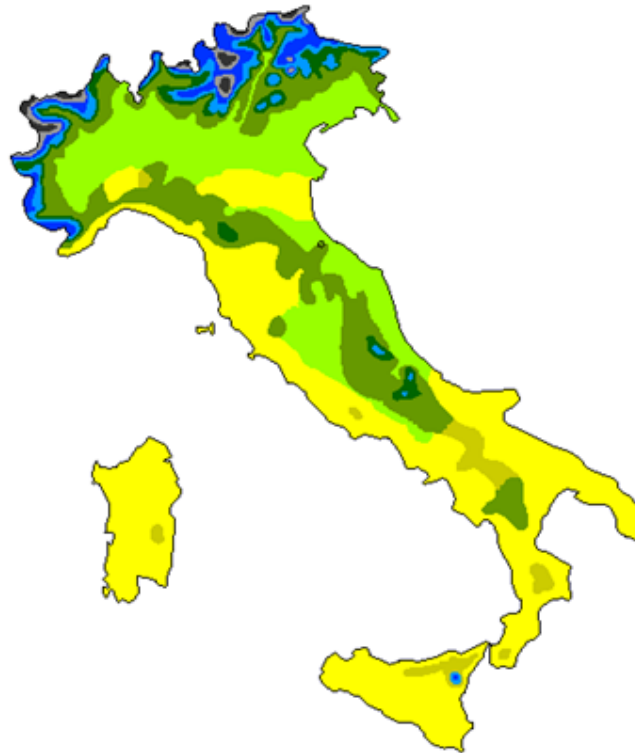


**Figure 2.1:** *Köppen climate classification map of Italy used for the preliminary selection of representative climatic regions [8]*

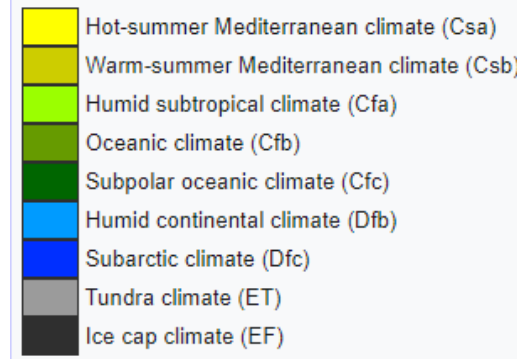


**Figure 2.2:** *Legend of the Köppen climate classification used in the Italian climatic analysis [8]*

The objective of this step was to ensure that the final selection included, as far as possible, at least one city for each climatic category present in Italy. However, the Italian territory does not encompass all Köppen climate types, and some of the existing classes occur only in highly mountainous or sparsely populated areas. These locations were excluded because they diverge significantly from the characteristics of the reference urban scenario of this study. Therefore, only cities whose climatic conditions were representative, scientifically meaningful, and compatible with the nature of the case study were retained.

This first screening based on climate and annual precipitation allowed for a preliminary group of candidate cities covering the main climatic variability across the country.

**Table 2.1:** *Representative Köppen climate types, associated cities, precipitation ranges, and data sources.*

<b>Köppen climate classification</b>	<b>City</b>	<b>Mean annual precipitation (mm)</b>	<b>Source</b>
Hot-summer Mediterranean (Csa)	Palermo, Grosseto, Roma	550–655–878	[9], [10], [11]
Warm-summer Mediterranean (Csb)	Potenza, San Giovanni in Fiore	625–708	[12], [13]
Humid subtropical (Cfa)	Torino, Ancona	1043–740	[14], [15]
Oceanic (Cfb)	Trento, Frontone	935–1158	[16], [15]
Subpolar oceanic (Cfc)	—	—	—
Subarctic (Dfc)	Sestriere	1363 (snow)	[14]

The second step of the selection procedure consisted of analysing the rainfall intensity and depth derived from the FOCA [17] project, which provides pixel-based hydrological parameters across the entire Italian territory. From the FOCA rasters, the  $a$  and  $n$  parameters of the intensity–duration equation were extracted for each candidate location using the QGIS Raster Calculator. These parameters were then used to compute both the 15-minute Mean ID value and the corresponding rainfall Depth, allowing for a consistent comparison among all cities.

This analysis made it possible to move beyond the simple consideration of annual precipitation and to identify locations with representative hydrological behaviour in terms of short-duration, high-intensity rainfall, which is relevant for urban drainage design and hydraulic invariance studies. The initial list of cities obtained from the Köppen classification was therefore complemented with FOCA-based intensity and depth values (Figure 2.3; Table 2.2 ), and those locations presenting atypically low or unrepresentative rainfall characteristics were excluded.

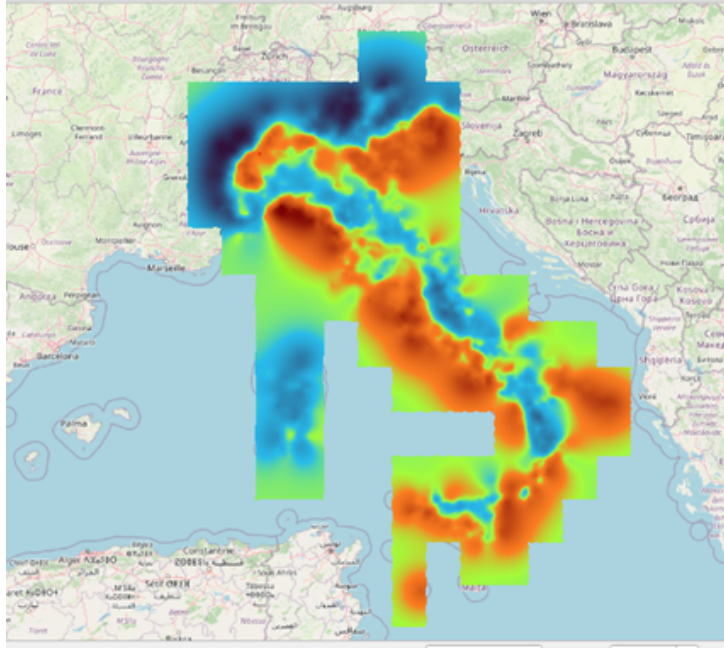


**Figure 2.3:** *FOCA raster dataset showing the spatial distribution of rainfall intensity parameters across Italy [17]*



**Table 2.2:** *FOCA-based rainfall intensity ( $I$ ) and depth ( $D$ ) values for candidate cities [17]*

City	$i$ (mm/h)	$D$ (mm)
<b>Torino</b>	22.4	5.5
<b>Palermo</b>	17.8	4.5
<b>Roma</b>	26.3	6.6
Grosseto	20.3	5.1
Ancona	18.3	4.6
Sestriere	7.6	1.9
Potenza	16.4	4.1
San Giovanni in Fiore	13.8	3.5
Trento	13.1	3.3
<b>Cagliari</b>	15.8	4.0
Sestri Levante	29.9	7.5
Santa Margherita di Liguria	31.0	7.8
Cosenza	13.3	3.3
<b>Palau</b>	12.1	3.0
Aosta	5.8	1.4
<b>Genova</b>	32.3	8.1

The first proposal of cities—derived from the climatic and precipitation screening—was then refined by selecting those with FOCA intensities and Depth values that were hydrologically meaningful and aligned with the objectives of the study, the relevant cities are: Turin, Palermo, Rome, Cagliari, Palau, and Genova. During this refinement, Palau emerged as an outlier due to its markedly lower intensity values compared to other locations. To maintain both hydrological representativeness and geographical diversity across Italy, Palau was replaced by Palermo, which shows FOCA-based rainfall characteristics consistent with the rest of the selected cities and belongs to a different geographical and climatic context. This substitution ensured that the final selection captured a balanced range of rainfall regimes while covering different Italian regions.

## 2.2 Selected Cities, Rainfall Conditions, and Groundwater Levels

### 2.2.1 Selected Cities

**Table 2.3:** *List of selected cities.*

City
Aosta
Cagliari
Palermo
Torino
Roma
Genova

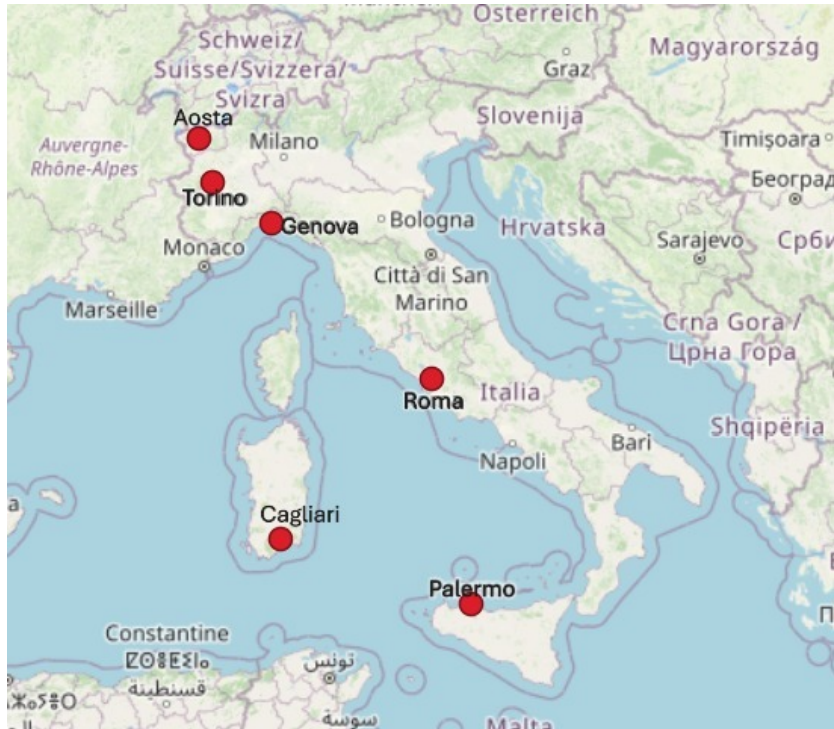


**Figure 2.4:** *Geographical location of the six selected Italian cities considered in the hydraulic invariance analysis: Torino, Genova, Aosta, Roma, Cagliari and Palermo*

### 2.2.2 Rainfall Data

Design rainfall values were obtained following the procedure detailed in Section 1.4.2 (Project Precipitation Calculation), where the complete methodology for computing storm depths and intensities for the selected return periods is described.

**Table 2.4:** *Design depth values for Duration = 15 min (mm) and for different return periods obtained using the GEV distribution*

City	T = 20 years	T = 30 years	T = 50 years
Aosta	9.1	9.6	10.2
Cagliari	27.0	28.6	30.7
Palermo	28.9	30.5	32.6
Torino	35.5	37.2	39.3
Roma	41.6	43.7	46.5
Genova	53.5	56.2	59.6
<b>Average</b>	<b>32.6</b>	<b>34.3</b>	<b>36.5</b>

**Table 2.5:** *Design depth values for Duration = 15 min (mm) and for different return periods obtained using the Gumbel distribution*

City	T = 20 years	T = 30 years	T = 50 years
Aosta	10.0	10.7	11.6
Cagliari	30.0	32.5	35.6
Palermo	31.9	34.4	37.6
Torino	38.8	41.6	45.2
Roma	45.7	49.0	53.2
Genova	58.8	63.4	69.2
<b>Average</b>	<b>35.9</b>	<b>38.6</b>	<b>42.0</b>

**Table 2.6:** *Design intensity values for Duration=15 min (mm/h) and for different return periods obtained using the GEV distribution*

City	T = 20 years	T = 30 years	T = 50 years
Aosta	36.4	38.3	40.7
Cagliari	108.1	114.5	122.7
Palermo	115.5	121.9	130.3
Torino	142.0	148.6	157.1
Roma	166.5	174.9	185.8
Genova	214.1	224.8	238.5
<b>Average</b>	<b>130.4</b>	<b>137.2</b>	<b>146.0</b>

**Table 2.7:** *Design intensity values for Duration=15 min (mm/h) and for different return periods obtained using the Gumbel distribution*

City	T = 20 years	T = 30 years	T = 50 years
Aosta	40.0	42.9	46.6
Cagliari	120.2	130.0	142.3
Palermo	127.7	137.7	150.2
Torino	155.1	166.5	180.7
Roma	182.7	196.1	212.8
Genova	235.3	253.7	276.7
<b>Average</b>	<b>143.6</b>	<b>154.4</b>	<b>168.0</b>

### 2.2.3 Groundwater Levels

For the six selected cities, detailed groundwater measurements at the exact project location were not available, as the study does not refer to a specific parcel within each urban area. To maintain methodological consistency across all locations, groundwater information was therefore obtained from official sources and technical studies reporting water table depths at representative points within high-density urban zones. This approach ensures that the adopted groundwater levels reflect conditions typical of consolidated metropolitan areas, allowing a coherent comparison among the six cities and aligning with the conceptual assumptions of the project-wide analysis.

**Table 2.8:** *Groundwater levels for the six selected cities, based on official hydrogeological sources.*

City	Groundwater Level (m)	Source
Aosta	17.0	[18]
Cagliari	2–10	[19]
Palermo	5.25	[20]
Torino	21.76	[21]
Roma	30.0	[22]
Genova	4.8–6.3	[23]

As shown in Table 2.8, the depth to groundwater varies significantly among the six selected cities. In particular, coastal cities such as Cagliari, Palermo and Genova exhibit shallow water tables, in some cases only a few meters below the surface. This behavior is fully consistent with the typical hydrogeological conditions of coastal plains, where the proximity to the sea, low topographic gradients and permeable alluvial deposits contribute to a reduced depth of the phreatic level. Conversely, inland cities such as Aosta, Torino and Roma present much deeper groundwater levels, reflecting their greater distance from the coast, higher elevations and more complex geological settings.

## 2.3 Construction Site and Characteristics

The selected case study corresponds to a hypothetical commercial development with an associated parking area, representative of common urban transformations considered in the framework of hydraulic and hydrologic invariance. The site is assumed to be located within an urban context, with flat to moderately sloping terrain and direct connection to the municipal drainage system. The main features of the site are summarized below, based on field survey observations and supplementary data from Google Maps/Earth.

### 2.3.1 Surface Types and Land Use

The main land-use components include:

**Table 2.9:** *Surface types and land use – construction site*

Surface type	Area (m <sup>2</sup> )	Percentage (%)
Building roof	11,914.7	56.4
Parking lot (concrete)	5,220.5	24.7
Sidewalks / Pedestrian areas	2,176.3	10.3
Green areas	1,823.3	8.6
<b>Total site area</b>	<b>21,134.8</b>	<b>100</b>

*Note: Areas were estimated using polygons drawn with the Google Earth Pro measurement tool [24].*



**Figure 2.5:** *Overview of the case study (Google Earth Pro) [24]*

### 2.3.2 Surface Materials

**Table 2.10:** *Surface types and materials – construction site*

Surface type	Notes
Building roof	flat reinforced concrete deck with water-proof membrane [25].
Parking lot (concrete)	Main impervious surface
Sidewalks / Pedestrian areas	Paved with concrete
Green areas	Decorative / pervious zones



**Figure 2.6:** *Parking lot surface*





**Figure 2.7:** *Sidewalk surface*



**Figure 2.8:** *Green areas*





**Figure 2.9:** *Green areas.*



**Figure 2.10:** *Green areas*

### 2.3.3 Slopes and Drainage Patterns

During the field visit, the general slope direction of the area was identified, along with visible low points and potential water accumulation zones. Slope measurements were taken using a mobile application [26] on different site sur-

faces. The sidewalks presented an average slope of approximately  $1^\circ$  and directed runoff towards the adjacent streets. The parking lot showed a slope of about  $1^\circ$ , which directed water towards an internal collector channel located within the lot. In addition, the vehicular access and exit ramps exhibited slightly steeper slopes, averaging  $2^\circ$ , guiding runoff efficiently towards the drainage system. These observations confirmed the overall drainage pattern.

### 2.3.4 Drainage System Details

A total of 26 stormwater inlets were identified along the perimeter of the mall, providing collection capacity for runoff generated on adjacent pedestrian and vehicular areas. Within the parking lot, a longitudinal collector channel was observed, designed to intercept and convey runoff from the paved surfaces towards the drainage system, thereby complementing the function of the perimeter inlets.



**Figure 2.11:** *stormwater inlet identified along the mall boundary*



**Figure 2.12:** *Collector channel located inside the parking lot*

# Chapter 3

## Results and Discussion

This chapter presents the outcomes derived from the methodology explained in Section 1.4.2

### 3.1 Calculation of the Design Storage Volume According to the Lombardy Regulation

In the present study, the selected case study does not correspond to a green-field development on a previously permeable area. The site is already fully urbanized, including buildings, parking lots, sidewalks, and other impermeable surfaces within a consolidated urban district. For this reason, the intervention can be classified under Case 6 (new construction derived from demolition/reconstruction or interventions within already urbanized areas), according to the [1]. In this case, the hydraulic invariance measures must be applied to the entire surface of the intervention, and the discharge is constrained to the regulatory outflow limit. This interpretation reflects the actual urban context of the site and ensures that the design of the storage tank complies with the most appropriate regulatory framework.

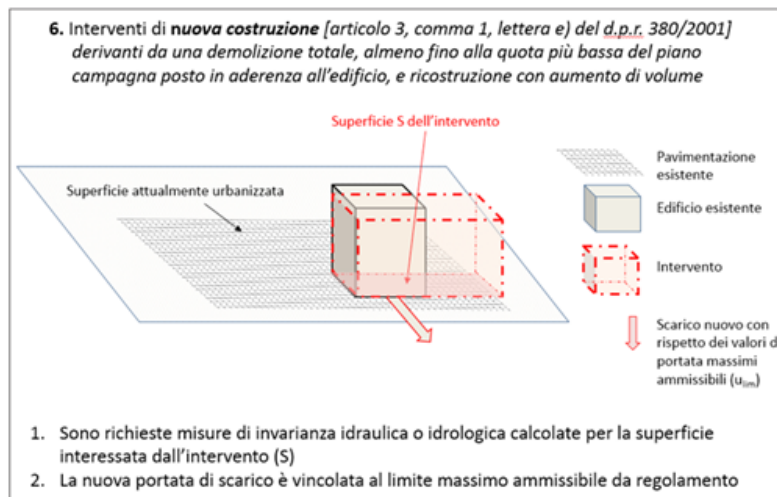


**Figure 3.1:** *Exemplary Scheme No. 6 of the interventions to which the hydraulic and hydrologic invariance measures must be applied, from Annex A [1]*

Since the study is applied to different cities across Italy, outside the Lombardy Region, it is not possible to classify the project area according to the categories defined by the Regional Regulation [1]. However, to evaluate the most critical scenario and to ensure uniformity in the comparison among all the analyzed locations, *Area A* (high hydraulic criticality) was assumed for every case. Consequently, the admissible outflow rate was set equal to  $u_{lim} = 10 \text{ l/s} \cdot \text{ha}$  for all the cities, ensuring that the design conditions remain consistent throughout the analysis.

For the application of hydraulic and hydrological invariance measures, the following runoff coefficients by land-use type were considered, in a simplified manner, as suggested by the regulation:

- Impermeable surfaces:  $\varphi = 1.0$
- Permeable surfaces:  $\varphi = 0.3$

By expressing the surfaces in hectares, the weighted average runoff coefficient was then calculated.

$$\varphi_m = \frac{(1.2 \text{ ha} \cdot 1) + (0.5 \text{ ha} \cdot 1) + (0.2 \text{ ha} \cdot 1) + (0.2 \text{ ha} \cdot 0.3)}{2.1 \text{ ha}} = 0.93 \quad (3.1)$$

With a total affected surface area equal to 2.1 ha and a weighted average runoff coefficient greater than 0.4, assuming Area A as the territorial context, the project falls into Intervention Class 3, i.e., high potential impermeabilization. Consequently, the detailed procedure must be adopted for the calculation of the storage volume.

CLASSE DI INTERVENTO	SUPERFICIE INTERESSATA DALL'INTERVENTO	COEFFICIENTE DEFUSSO MEDIO PONDERALE	MODALITÀ DI CALCOLO	
			AMBITI TERRITORIALI (articolo 7)	
			Aree A, B	Aree C
0	Impermeabilizzazione potenziale qualsiasi	$\leq 0,03 \text{ ha}$ ( $\leq 300 \text{ mq}$ )	qualsiasi	Requisiti minimi articolo 12 comma 1
1	Impermeabilizzazione potenziale bassa	da $> 0,03 \text{ a} \leq 0,1 \text{ ha}$ (da $> 300 \text{ a} \leq 1.000 \text{ mq}$ )	$\leq 0,4$	Requisiti minimi articolo 12 comma 2
2	Impermeabilizzazione potenziale media	da $> 0,03 \text{ a} \leq 0,1 \text{ ha}$ (da $> 300 \text{ a} \leq 1.000 \text{ mq}$ )	$> 0,4$	Metodo delle sole piogge (vedi articolo 11 e allegato G)  Requisiti minimi articolo 12 comma 2
		da $> 0,1 \text{ a} \leq 1 \text{ ha}$ (da $> 1.000 \text{ a} \leq 10.000 \text{ mq}$ )	qualsiasi	
		da $> 1 \text{ a} \leq 10 \text{ ha}$ (da $> 10.000 \text{ a} \leq 100.000 \text{ mq}$ )	$\leq 0,4$	
3	Impermeabilizzazione potenziale alta	da $> 1 \text{ a} \leq 10 \text{ ha}$ (da $> 10.000 \text{ a} \leq 100.000 \text{ mq}$ )	$> 0,4$	Procedura dettagliata (vedi articolo 11 e allegato G)
		$> 10 \text{ ha}$ ( $> 100.000 \text{ mq}$ )	qualsiasi	

**Figure 3.2:** Table A of the Regional Regulation of Lombardy (R.R. Lombardia) 19 April 2019 [1]



The calculations and results of the design precipitation for each selected city are presented in Section 2.2.2. This section summarizes the adopted parameters and methodological choices.

As explained in Section 1.4.2, the regional regulation [1] requires that the feasibility of infiltration must be evaluated based on the local geological and hydrogeological conditions, such as soil permeability, groundwater level, and the presence of impermeable or contaminated layers. In the absence of specific geotechnical investigations or reliable soil data, the regulation prescribes that infiltration cannot be considered in the design process. Consequently, for the present study—which aims to apply the Lombardy regulation to different Italian cities without detailed subsoil characterization—only detention (lamination) storage was considered, while infiltration was excluded from the analysis. This conservative assumption ensures compliance with the regulation and allows for a consistent comparison of results among the selected study cases.

According to Article 11 of [1] and Annex G, the design rainfall must be represented by a Chicago hyetograph whose total duration exceeds the catchment concentration time. The regulation specifies a peak position of  $r = 0.4$ . In this study, a 30-minute design duration was adopted, which is longer than the computed concentration time of the urban lot and thus fully compliant with the regulatory prescription. This duration also aligns with the examples provided in the regional guidelines.

The parameters  $a$  and  $n$  were obtained from the FOCA database [17], while the growth factor  $K_{50}$  was computed through a GEV analysis based on L-moments, following the procedure of Hosking and Wallis [5]. In the FOCA framework, the design growth factor  $K_T$  is derived from regional L-moment ratios (LCV and LCA), which are assumed to be invariant with respect to storm duration. Consequently,  $K_T$  depends solely on the statistical properties of the regional GEV distribution and not on rainfall duration. Therefore, the same  $K_{50}$  values obtained for 15-minute storms were retained for the 30-minute design duration, ensuring full consistency with the regional FOCA methodology.

**Table 3.1:** *Parameters of the rainfall curves for each city*

City	$a$	$n$	$K_{50}$
Aosta	11.54	0.50	1.77
Cagliari	22.37	0.28	2.02
Palermo	25.89	0.29	1.87
Torino	32.00	0.26	1.76
Roma	34.33	0.23	1.86
Genova	50.82	0.33	1.85

Based on the parameters mentioned above, the following hyetograph is obtained, distributed over a period of 30 minutes with a time step of 1 minute.

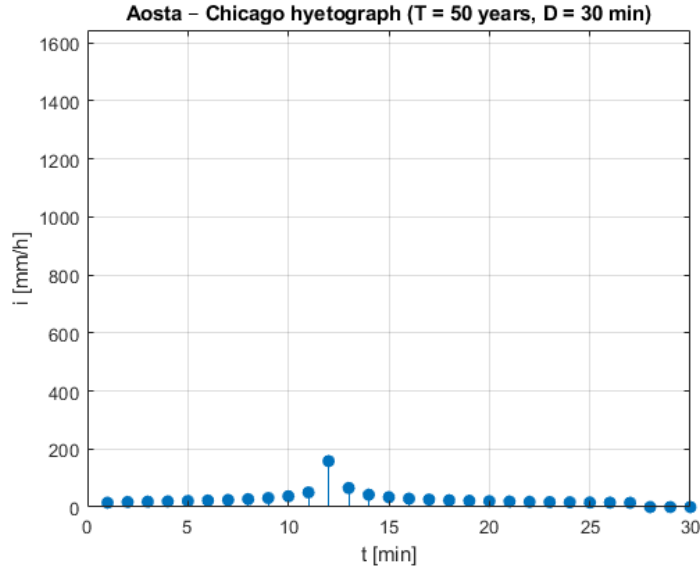


**Figure 3.3:** *Chicago hyetograph with a duration of 30 minutes and a return period of 50 years, for the city of Aosta*

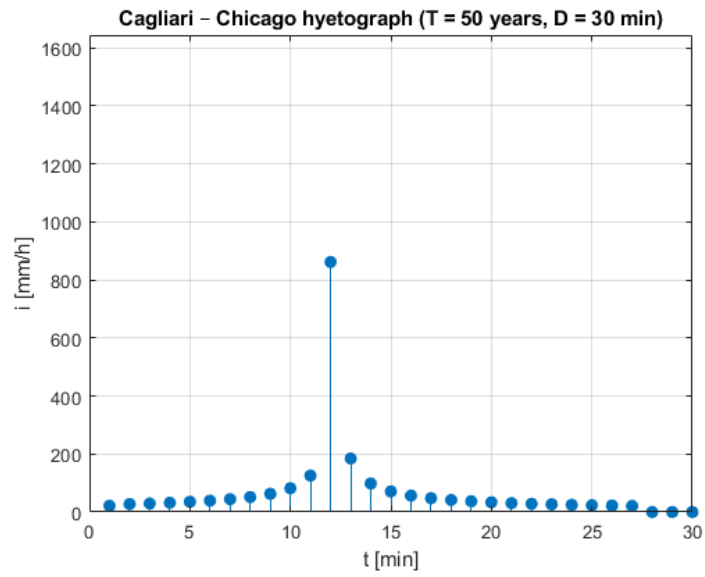


**Figure 3.4:** *Chicago hyetograph with a duration of 30 minutes and a return period of 50 years, for the city of Cagliari*

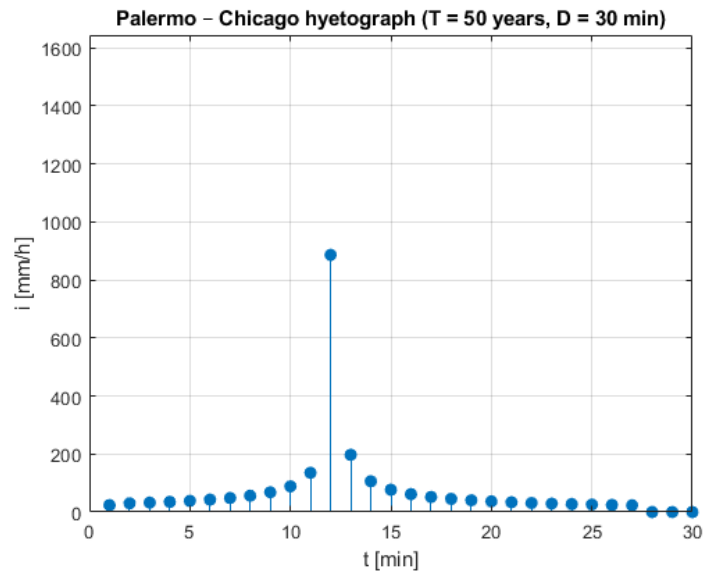


**Figure 3.5:** *Chicago hyetograph with a duration of 30 minutes and a return period of 50 years, for the city of Palermo*



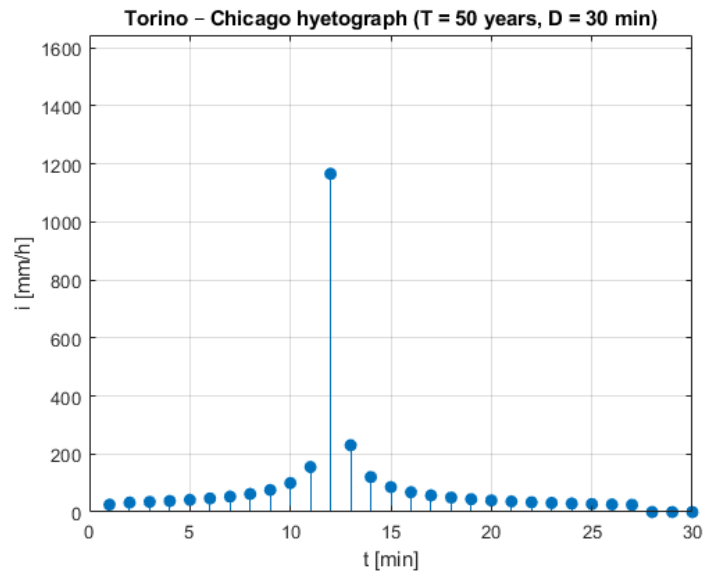


**Figure 3.6:** *Chicago hyetograph with a duration of 30 minutes and a return period of 50 years, for the city of Torino*

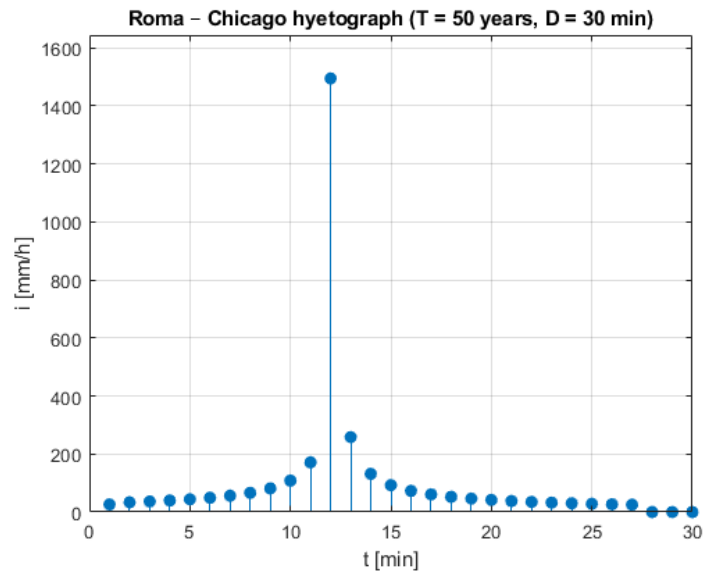


**Figure 3.7:** *Chicago hyetograph with a duration of 30 minutes and a return period of 50 years, for the city of Roma*

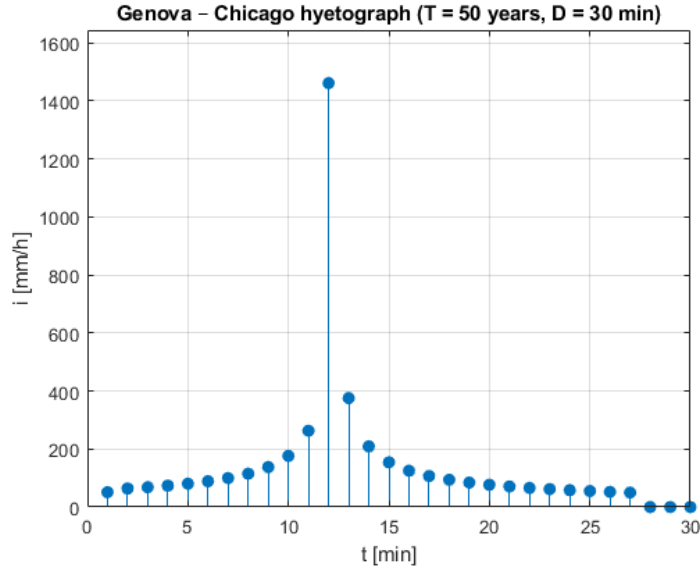


**Figure 3.8:** *Chicago hyetograph with a duration of 30 minutes and a return period of 50 years, for the city of Genova*

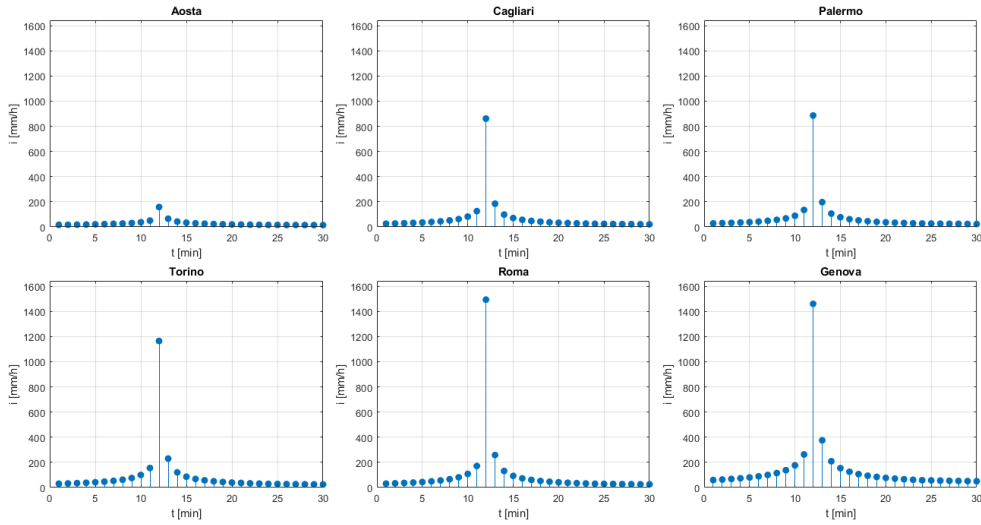


**Figure 3.9:** *Comparison of the 30-minute design Chicago hyetographs ( $T = 50$  years,  $r = 0.4$ ) for the six study sites. The different peak intensities highlight the spatial variability of short-duration rainfall across Italy.*

According to the example provided in Annex H, the concentration time ( $t_c$ ) for each subarea was selected by considering not only the degree of surface

impermeability but also the flow path length and the local drainage configuration. Consequently, a value of  $t_c = 15$  minutes was adopted for impervious roofs and terraces, where runoff travels through gutters and downpipes before reaching the drainage network;  $t_c = 10$  minutes was assumed for parking areas and pavements, characterized by shorter and more direct flow paths; and  $t_c = 12$  minutes was assigned to the green areas, which are small and directly connected to the stormwater system, neglecting infiltration but maintaining a slightly longer response time due to surface roughness. Figure 3.10 illustrates the adopted subdivision of the catchment into three sub-basins (mall, parking lot, and green area) and their respective drainage directions toward the detention tank.

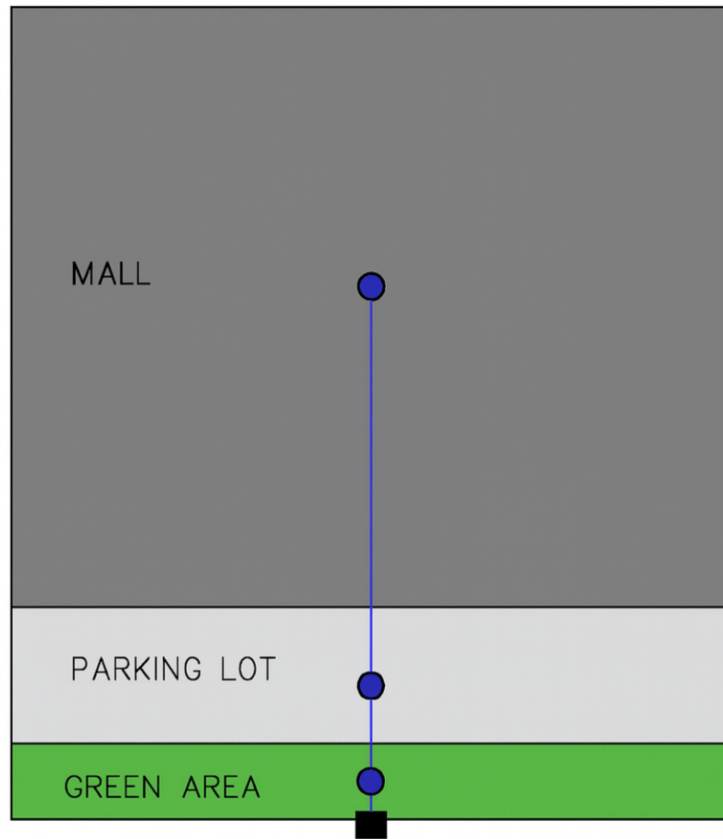


**Figure 3.10:** *Sub-basins scheme*

From these data, the inflow hydrograph was derived by calculating the

discharge  $Q_i(t)$  [ $\text{m}^3/\text{s}$ ] as:

$$Q_i(t) = \frac{i(t)}{1000 \cdot 3600} \cdot A_i \cdot \varphi_i$$

$i(t)$  is the rainfall intensity from the hyetograph,  $A_i$  the area of the  $i$ -th sub-catchment (see Table 2.9), and  $\varphi_i$  the runoff coefficient of the  $i$ -th sub-catchment.

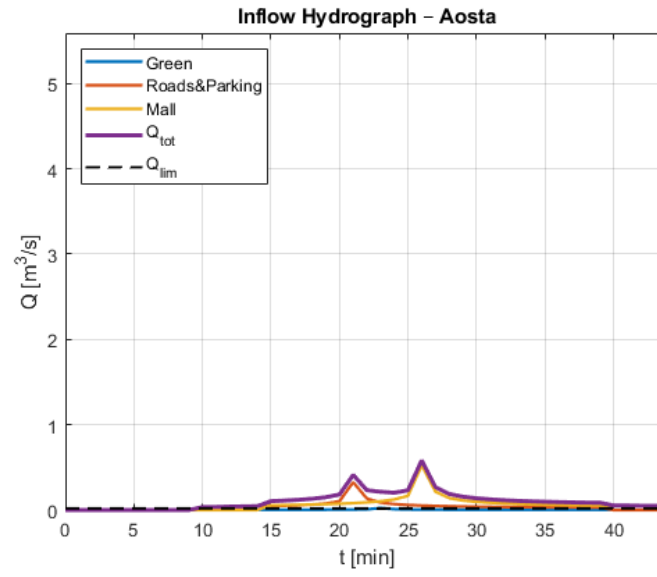


**Figure 3.11:** *Inflow Hydrograph – Aosta*

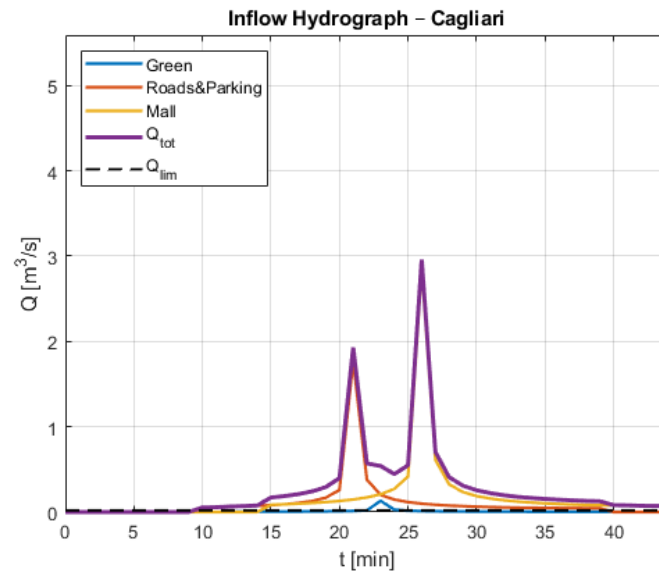


**Figure 3.12:** *Inflow Hydrograph - Cagliari*

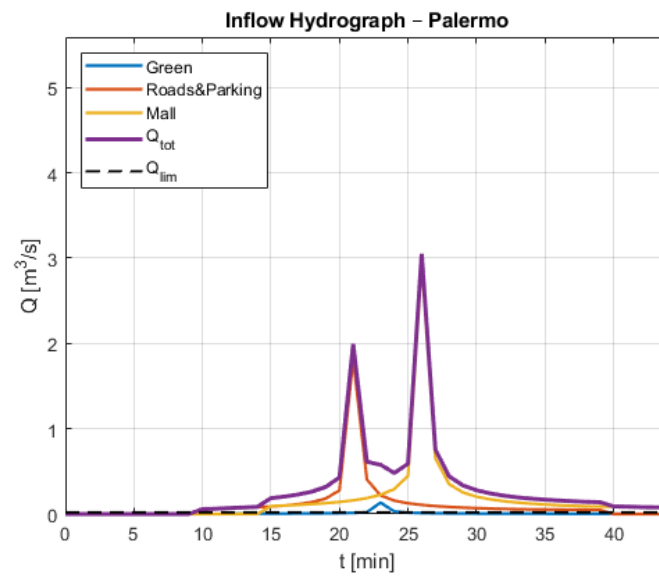


**Figure 3.13:** *Inflow Hydrograph - Palermo*

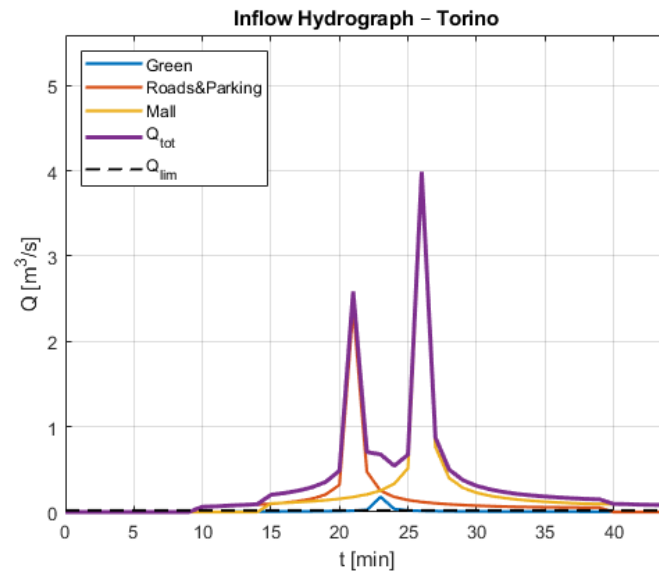


**Figure 3.14:** *Inflow Hydrograph - Torino*

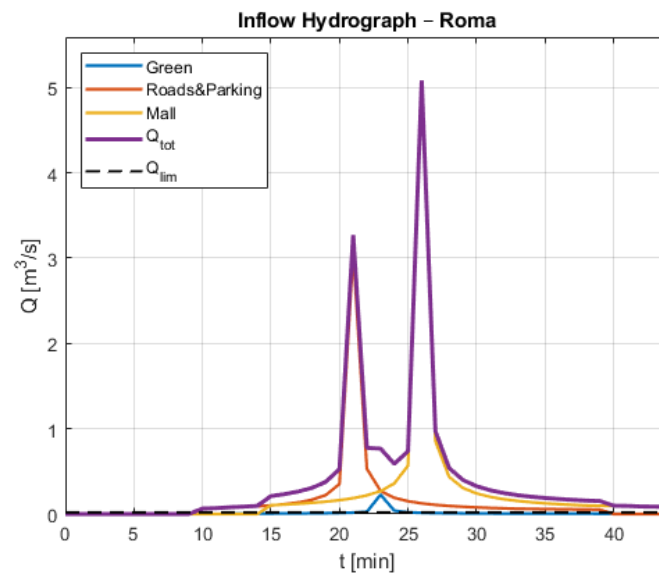


**Figure 3.15:** *Inflow Hydrograph - Roma*

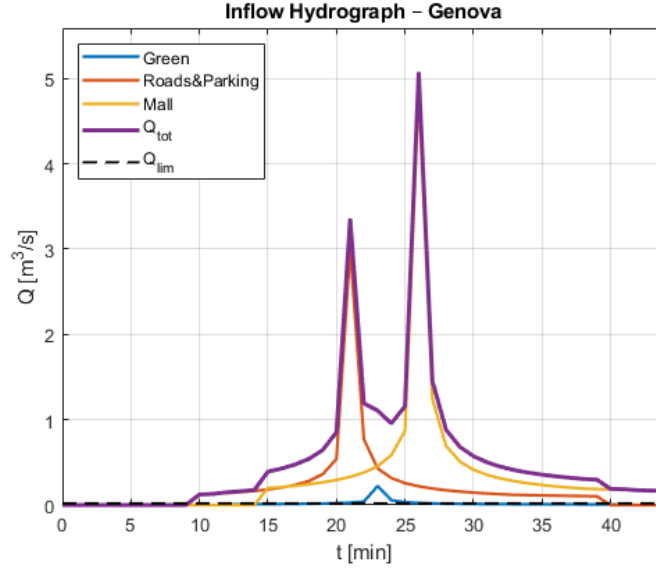


**Figure 3.16:** *Inflow Hydrograph – Genova*

**Table 3.2:** *Peak inflow discharge obtained for each study city*

City	$Q_{peak}$ [m <sup>3</sup> /s]
Aosta	0.6
Cagliari	2.9
Palermo	3.1
Torino	4.0
Roma	5.1
Genova	5.1

As shown in Table 3.2, the peak inflow discharges obtained for all cities exceed the maximum admissible outflow equal to  $Q_{lim} = 0.02\text{m}^3/\text{s}$ . This confirms that detention measures are required to reduce the outlet flow below the regulatory threshold.

The equivalent impervious area was computed as:

$$A_{imp,eq} = \frac{\sum_i A_i \varphi_i}{10^4} = 2.0 \quad [\text{ha}], \quad (3.2)$$

and the maximum allowable outflow as:

$$Q_{lim} = U_{max} A_{imp,eq}, \quad U_{max} = 10 \frac{l}{s \cdot \text{ha}} = 0.01 \frac{m^3}{s \cdot \text{ha}}. \quad (3.3)$$

The exceedance volume was integrated over a time step of  $\Delta t = 60$  s, as:

$$V_{det} = \sum_t \max(0, Q_{tot}(t) - Q_{lim}) \Delta t, \quad v = \frac{V_{det}}{A_{imp,eq}} [\text{m}^3/\text{ha}]. \quad (3.4)$$

According to the regional regulation [1], the minimum required volume is:

$$V_{min} = 800 \frac{\text{m}^3}{\text{ha}} \cdot P \cdot A_{imp,eq}, \quad (3.5)$$

where  $P$  is a correction factor derived from Annex C (if not available,  $P = 1$ ). Finally, the design storage volume is given by:

$$V_{proj} = \max(V_{det}, V_{min}). \quad (3.6)$$

Applying this procedure to each city yields the results shown in Table 3.3.

**Table 3.3:** *Detention volumes obtained for each study city*

City	$V_{det}$ [ $\text{m}^3$ ]	$v$ [ $\text{m}^3/\text{haimp}$ ]	$V_{proj}$ [ $\text{m}^3$ ]
Aosta	245.1	123.4	1588.7
Cagliari	697.3	351.2	1588.7
Palermo	744.7	375.0	1588.7
Torino	892.3	449.3	1588.7
Roma	1039.5	523.4	1588.7
Genova	1443.6	726.9	1588.7

As shown in Table 3.3, the specific detention volumes  $v$  obtained for all cities are lower than the minimum regulatory value of  $800 \text{ m}^3/\text{haimp}$  prescribed for highly critical areas. Consequently, the total design detention volume for each case was set to  $V_{proj} = 1588.7 \text{ m}^3$ , ensuring compliance with the minimum standard established by the regional regulation.

With no infiltration, the emptying time is

$$T_{empty} = \frac{V_{proj}}{Q_{lim}}, \quad Q_{lim} = U_{max} P A_{imp,eq},$$

with  $U_{max} = 10 \text{ L s}^{-1} \text{ ha}^{-1}$  (Area A). For the present case,  $V_{proj} = 1588.7 \text{ m}^3$  and  $Q_{lim} = 19.86 \text{ L/s}$ , yielding  $T_{empty} \approx 22.2 \text{ h}$  ( $< 48 \text{ h}$ ).



## 3.2 Stormwater Detention System Design

### 3.2.1 Proposed SuDS Solution Based on Modular Geocellular Structures

After determining the required storage volume according to the regulatory method, the next step is to define the stormwater management solution to be adopted within the study area. The selected configuration accounts for the hydraulic results obtained, as well as the morphological and spatial characteristics of the site, ensuring a technically feasible and regulation-compliant design.

Since the same case-study configuration was applied in all cities and the resulting detention volume was identical ( $V_{proj} = 1588.7 \text{ m}^3$ ), a single design solution was developed and considered representative for all scenarios. This unified approach allows for a direct comparison between cities based solely on their rainfall characteristics, while maintaining a consistent storage configuration.

As infiltration was not considered in this study, the proposed system operates exclusively through a controlled outflow to the sewer network, limited to the maximum admissible discharge prescribed by the Lombardy Regulation ( $Q_{lim} = 10 \text{ L s}^{-1} \text{ ha}^{-1}$ ). The facility therefore functions as a detention system designed to temporarily attenuate peak flows and ensure compliance with the regulatory outflow constraint.

Traditionally, stormwater detention can be achieved through natural or purpose-built depressed areas designed to temporarily retain runoff. These basins may incorporate bottom outlets for controlled emptying, overflow structures for extreme events, and either impermeable or permeable bases depending on site-specific conditions. Impermeable bases are typically recommended when groundwater is shallow or when there is a potential risk of contaminating the underlying aquifer.

However, in high-density urban environments, open surface basins are often impractical due to space limitations. For this reason, the present study adopts a subsurface solution based on modular geocellular storage systems. These systems are composed of lightweight, high-void ratio structural units capable of providing the required detention volume while remaining fully integrated underground. Their modular nature offers substantial design flexibility, enabling adaptation to irregular footprints and constrained urban geometries. Additionally, when appropriately engineered, geocellular systems can withstand vehicular loads, allowing installation beneath parking lots, roads, and pedestrian areas without affecting surface usability. Such systems

are widely employed in contemporary SuDS applications and recommended by specialized manufacturers such as [27].

In this study, the selected configuration corresponds to a subsurface detention basin constructed using geocellular modular units. Although the system includes a permeable internal base to allow water to freely enter the geocellular modules, the entire structure is enclosed within an impermeable external membrane. This ensures that no infiltration occurs into the surrounding soil and that the stored volume is used exclusively for temporary detention prior to controlled discharge to the public sewer network.

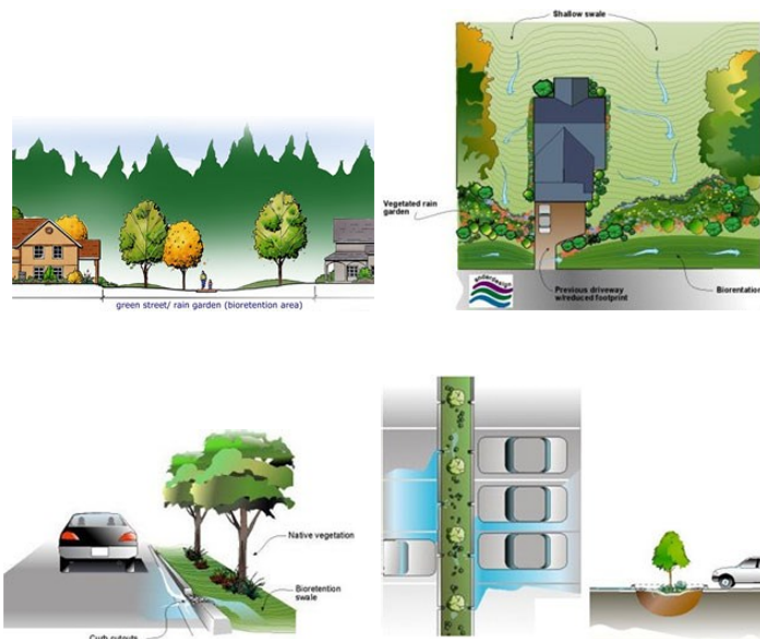


**Figure 3.17:** *Proposed retention/lamination area schemes in LID systems [1]*



**Figure 3.18:** *Examples of surface laminating structures consisting of open-air basins and channels [1]*



**Figure 3.19:** *Examples of surface laminating structures consisting of open-air basins and channels [1]*



**Figure 3.20:** *Example of a geocellular SuDS detention system during a storm event, showing temporary subsurface water storage. Image courtesy of [27].*



**Figure 3.21:** *Installation phase of a geocellular modular system for subsurface stormwater detention. The modular units provide high storage capacity and structural strength. Image courtesy of [27].*

### 3.2.2 Hydraulic Design

The proposed solution consists of a fully integrated stormwater conveyance and detention system that collects runoff from both the building roof and the parking area, directing it toward the subsurface geocellular storage units. Rainfall falling on the roof is first captured through the designed network of roof drains and conveyed vertically through downpipes. These downpipes discharge into the horizontal conveyance system, where the flow is combined with the runoff generated on the parking lot surface.

Runoff from the paved parking area is collected through a longitudinal surface channel. This channel divides the inflow into two equal branches, each of which is directed toward a dedicated first-flush treatment unit. These units remove the initial pollutant load associated with early rainfall before the flow is admitted into the detention system.

Following treatment, each stream is conveyed to one of the two existing open detention basins located within the site's green area. Beneath these basins, the subsurface modular geocellular structures provide the required detention volume. The geocellular modules are filled by gravity through the

permeable internal base of the basins, while the outer envelope of the system remains impermeable to prevent infiltration into the surrounding soil.

After temporary storage, the detained water is discharged into the public sewer network through a controlled outflow system. Since the site does not permit gravity discharge, a pumping unit ensures that the release occurs only once the detention function has been fulfilled and always respecting the regulatory outflow limit.

The complete system configuration, together with the associated hydraulic calculations, was developed in accordance with the design principles and recommendations provided in the CIRIA SuDS Manual [28]. The following sections present the detailed hydraulic sizing and design assumptions adopted for each component.

### **Roof drains and vertical downpipes**

Given the roof area of 11 914.7 m<sup>2</sup>, the surface was subdivided into 40 drainage modules, each of approximately 298 m<sup>2</sup>. The design rainfall intensity was derived from the most critical city, Genova, which exhibits the highest 15-minute intensity for a 50-year return period (Table 2.6), namely  $i_{\text{crit}} = 238.5 \text{ mm h}^{-1}$ . Using the Rational Method,

$$Q = C i A,$$

with  $C = 1.0$ , the peak discharge per drain becomes:

$$Q_{\text{sum}} = \frac{i_{\text{crit}} A}{3.6 \times 10^6} = \frac{238.5 \times 298}{3.6 \times 10^6} \approx 0.0197 \text{ m}^3 \text{ s}^{-1}.$$

Since vertical downpipes operate under full-flow conditions, their diameter is obtained using the continuity equation:

$$Q = v \frac{\pi D^2}{4},$$

with a design velocity of  $v = 2 \text{ m s}^{-1}$ . Solving for  $D$  yields an internal diameter of  $D \approx 0.112 \text{ m}$ , for which the adopted commercial size is DN 125 mm.

### **Horizontal roof collector pipes**

The pipes that collect and route flow from multiple roof drains were sized using Manning's equation for circular conduits flowing full:

$$Q = \frac{1}{n} A R^{2/3} S^{1/2},$$

with  $n = 0.011$  (PVC pipes),  $R = D/4$ , and a slope of  $S = 0.01$ . The required diameters depend on the number of contributing drains:

Number of drains	$Q$ ( $\text{m}^3 \text{s}^{-1}$ )	$D_{\text{adopted}}$ (mm)
1	0.0197	DN 160
2	0.0395	DN 250
3	0.0592	DN 250
5	0.0987	DN 300

These diameters result in full-flow velocities typically between about 0.8 and  $1.4 \text{ m s}^{-1}$ , which are compatible with self-cleansing criteria for smooth stormwater pipes.

#### **Main vertical downpipes**

Since the roof drainage system includes a total of 40 roof drains, these were grouped in sets of five in order to reduce the number of vertical discharge points along the building façade. This results in a total of

$$\frac{40}{5} = 8$$

main vertical downpipes.

For each downpipe, the combined discharge corresponds to the contribution of five roof drains:

$$Q_{\text{main}} = 5 Q_{\text{sum}} = 5 \times 0.0197 \approx 0.0987 \text{ m}^3 \text{s}^{-1}.$$

Using the continuity equation

$$Q = v \frac{\pi D^2}{4},$$

with a design velocity of  $v = 2 \text{ m s}^{-1}$ , the required hydraulic diameter is

$$D = \sqrt{\frac{4Q_{\text{main}}}{\pi v}} \approx 0.251 \text{ m},$$

for which the selected commercial size is DN 250 mm. The final horizontal collector was sized as DN 300 mm based on Manning's equation and the available slope (1%), whereas the corresponding main vertical downpipe was sized as DN 250 mm using the continuity equation, since vertical flow is not slope-controlled and higher velocities are acceptable.

#### **Parking lot drainage channel**

Runoff from the paved surface is collected by a longitudinal surface channel that extends for a total length of 102.7 m. The channel reaches its highest

point approximately at mid-length, where the watershed divide is located. From this point, the channel splits into two branches of equal length (roughly 51.35 m each), directing the runoff toward the two independent first-flush treatment units positioned on the right and left sides of the site.

Each branch was designed with its own longitudinal slope so that the runoff is symmetrically conveyed toward the corresponding treatment unit. For a branch length of 51.35 m, the recommended design slopes are:

$$\begin{aligned} S = 1\% & \Rightarrow \Delta z = 0.51 \text{ m}, \\ S = 0.5\% & \Rightarrow \Delta z = 0.26 \text{ m}, \\ S = 0.3\% & \Rightarrow \Delta z = 0.15 \text{ m}. \end{aligned}$$

Given the project's geometric constraints, a longitudinal slope of 0.5% was selected for both branches, as it provides an optimal balance between hydraulic performance, self-draining capacity, and compatibility with the existing site elevations.

#### **Runoff distribution toward the first-flush treatment units**

To determine the discharge conveyed to each of the two first-flush treatment units, the contributing flows from both the roof and the parking area were evaluated using the Rational Method. The same design rainfall intensity used in the sizing of the roof drainage system was adopted, namely  $i_{\text{crit}} = 238.5 \text{ mm h}^{-1}$ .

*Roof runoff contribution* With a total roof area of  $A_{\text{roof}} = 11\,914.7 \text{ m}^2$  and a runoff coefficient  $C_{\text{roof}} = 1.0$ , the peak discharge generated on the roof is:

$$Q_{\text{roof,tot}} = \frac{C_{\text{roof}} i_{\text{crit}} A_{\text{roof}}}{3.6 \times 10^6} = \frac{1.0 \times 238.5 \times 11\,914.7}{3.6 \times 10^6} \approx 0.789 \text{ m}^3 \text{ s}^{-1}.$$

Since the site layout divides the roof drainage network symmetrically into two halves, each branch receives:

$$Q_{\text{roof,side}} = \frac{Q_{\text{roof,tot}}}{2} \approx 0.395 \text{ m}^3 \text{ s}^{-1}.$$

*Parking area runoff contribution* The paved parking area covers  $A_{\text{carpark}} = 5220.5 \text{ m}^2$ , with an assumed runoff coefficient of  $C_{\text{carpark}} = 1.0$  due to its impervious surface. The corresponding peak discharge is:

$$Q_{\text{carpark,tot}} = \frac{C_{\text{carpark}} i_{\text{crit}} A_{\text{carpark}}}{3.6 \times 10^6} = \frac{1.0 \times 238.5 \times 5220.5}{3.6 \times 10^6} \approx 0.346 \text{ m}^3 \text{ s}^{-1}.$$

Given that the longitudinal surface channel is divided by a central high point, the surface runoff is split evenly between the right and left branches:

$$Q_{\text{carpark,side}} = \frac{Q_{\text{carpark,tot}}}{2} \approx 0.173 \text{ m}^3 \text{ s}^{-1}.$$

*Total discharge toward each first-flush treatment unit* By combining the contributions from the roof and the parking area, the total flow conveyed to each side of the system is:

$$Q_{\text{side}} = Q_{\text{roof,side}} + Q_{\text{carpark,side}} \approx 0.395 + 0.173 \approx 0.568 \text{ m}^3 \text{ s}^{-1}.$$

This discharge is routed to a dedicated inspection chamber located at the end of each branch of the surface channel. Within each chamber, the roof runoff conveyed by the vertical downpipes and the surface runoff carried by the drainage channel combine before entering the corresponding first-flush treatment unit. In this way, each of the two parallel treatment lines receives a balanced inflow of approximately  $0.568 \text{ m}^3 \text{ s}^{-1}$ , ensuring uniform hydraulic loading and effective pre-treatment of polluted initial runoff prior to its admission into the detention basins.

It is important to distinguish between the design flow rate associated with the extreme storm event used for hydraulic sizing and the flow rate that actually requires water-quality treatment. In this study, the peak inflow to each branch of the system during the design storm with a 50-year return period is approximately  $Q_{\text{side}} = 0.568 \text{ m}^3 \text{ s}^{-1}$  (i.e.  $568 \text{ L s}^{-1}$ ), resulting from the combined contribution of roof and parking-lot runoff under the critical intensity  $i_{\text{crit}} = 238.5 \text{ mm h}^{-1}$ .

The pipe connecting the inspection chamber to the first-flush treatment unit was designed to convey the full peak inflow generated during the 50-year design storm, equal to  $Q_{\text{side}} = 0.568 \text{ m}^3 \text{ s}^{-1}$ . Because this pipe operates under gravity but with a full cross-section—due to the water level inside the chamber rising above the pipe crown—it was sized using the continuity equation rather than Manning’s formula. Assuming a representative design velocity of approximately  $v = 2 \text{ m s}^{-1}$ , which is widely accepted for stormwater conduits, the required hydraulic diameter is:

$$D = \sqrt{\frac{4Q_{\text{side}}}{\pi v}} = \sqrt{\frac{4 \times 0.568}{\pi \times 2}} \approx 0.60 \text{ m},$$

leading to the adoption of a DN 600 mm pipe.

Although a velocity of  $2 \text{ m s}^{-1}$  may appear relatively high, it lies well within the acceptable range for gravity-driven stormwater conduits. According to the [28], full-flow velocities of up to 2–3 m/s are permissible in closed pipes, provided that the conduit is short and the transported material is not prone to causing abrasion—conditions that are fully met in this project. The selected conduit is constructed in high-density polyethylene (HDPE/PEAD), whose smooth internal surface, high abrasion resistance, and structural flexibility make it particularly suited for stormwater applications involving elevated velocities. Larger diameters (e.g. DN 800 or DN 1000 mm) would



reduce the velocity to about 1.1–0.7 m/s but would significantly increase excavation depth and construction cost without offering substantial functional advantages. For these reasons, DN 600 mm represents the most appropriate and efficient solution.

In accordance with [28], the runoff requiring specific water-quality treatment is associated with relatively small rainfall depths, typically in the order of 10–15 mm. For this project, a design rainfall depth of 15 mm was adopted for the sizing of the first-flush treatment units. Consistently with the 30-minute design storm duration used in the hydraulic analysis, this depth was represented as a uniform intensity of

$$i_{\text{treat}} = \frac{15 \text{ mm}}{0.5 \text{ h}} = 30 \text{ mm h}^{-1}.$$

The total impervious area contributing to the system is

$$A_{\text{tot}} = A_{\text{roof}} + A_{\text{carpark}} = 11\,914.7 + 5220.5 = 17\,135.2 \text{ m}^2,$$

which is divided symmetrically between the two branches:

$$A_{\text{side}} = \frac{A_{\text{tot}}}{2} = 8567.6 \text{ m}^2.$$

Using the Rational Method,

$$Q = \frac{C i A}{3.6 \times 10^6},$$

with a runoff coefficient  $C = 1.0$ , the design treatment flow for each line is:

$$Q_{\text{treat,side}} = \frac{1.0 \times 30 \times 8567.6}{3.6 \times 10^6} \approx 0.0714 \text{ m}^3 \text{ s}^{-1} \approx 71 \text{ L s}^{-1}.$$

Therefore, while each branch is hydraulically capable of conveying up to  $0.568 \text{ m}^3 \text{ s}^{-1}$  during the 50-year design storm, only the portion of the flow corresponding to the 15 mm water-quality event—approximately  $0.071 \text{ m}^3 \text{ s}^{-1}$  (71 L/s)—is considered to require first-flush treatment in line with the guidance [28]. For design and construction purposes, this value was rounded to 75 L/s, providing a conservative margin and facilitating the specification of treatment units and associated conveyance elements. The remaining flow bypasses the treatment units and is managed primarily by the downstream detention system, whose role is the attenuation of peak discharges and compliance with regulatory outflow limits.

The first-flush treatment units adopted in this project are prefabricated reinforced-concrete tanks (“vasche di prima pioggia”), designed in accordance

with Italian environmental legislation. The legal framework governing the treatment of first-flush runoff is established primarily by the *Decreto Legislativo 3 aprile 2006, n. 152* (Testo Unico Ambientale), which distinguishes between ordinary stormwater runoff and the more polluted initial portion of rainfall (prima pioggia) that requires dedicated treatment [29]. Additional technical criteria are provided by regional regulations, such as the *D.G.R. Lombardia 7/18532/2004* [30] and the *D.G.R. Piemonte 46-11968/2012* [31], which define first-flush depths, treatment requirements, and typical design configurations for facilities serving parking areas, commercial surfaces, and other impervious zones. In accordance with these regulations, the reinforced-concrete first-flush units adopted in this project ensure adequate separation and pre-treatment of the polluted initial runoff before the remaining flow is conveyed to the downstream detention system.

The first-flush treatment tank is installed beneath the parking area and its burial depth was defined by combining structural, hydraulic and operational criteria. As recommended for underground SuDS components located beneath trafficked surfaces, a minimum soil cover is required to ensure adequate structural resistance to wheel loads, to prevent localised deformation of the tank roof, and to provide sufficient bedding and backfill layers. For parking areas subjected to light-to-moderate traffic, a soil cover in the order of 0.7–1.0 m above the tank crown is typically adopted. In this project, a cover depth of approximately 0.8 m was selected, consistent with the loading conditions and the anticipated pavement structure.

In addition to structural considerations, the installation depth also had to accommodate the hydraulic levels of the incoming and outgoing pipelines. The tank was therefore positioned such that the inflow from both the roof drainage system and the parking-lot channel enters by gravity, while still maintaining sufficient elevation to allow controlled discharge towards the downstream detention system. Finally, the adopted depth ensures proper access for inspection and maintenance through surface manholes, while avoiding undesirable interaction with the groundwater table, which could otherwise increase external uplift forces or compromise long-term stability. This combination of structural, hydraulic and operational requirements establishes a robust and practical installation depth for the first-flush treatment unit.

### **Combined Detention Basin and Geocellular Storage System**

The inlet pipe discharging into the detention basin was positioned so that its invert lies slightly above the basin floor in order to prevent sediment re-entrainment and minimise local scouring at the point of discharge. Given the adopted basin floor elevation of  $z_f = -1.20$  m and the pipe diameter of 600 mm, the pipe invert level was set 0.15 m above the basin bot-

tom, i.e. at  $z_{\text{invert}} = -1.05$  m. This results in a pipe centreline elevation of  $z_{\text{centre}} = -0.75$  m and a crown elevation of  $z_{\text{crown}} = -0.45$  m. The adopted configuration ensures that the pipe remains submerged during basin operation, while maintaining full gravitational inflow consistency with the upstream conveyance system and avoiding interference with the maximum water level in the detention basin.

### **Detention basin configuration and surface design**

The detention basins were designed in accordance with the principles described in Chapter 22 of the [28], which provides guidance on the geometry, safety requirements and construction details of shallow storage basins. Following these recommendations, a horizontal safety margin of approximately 1 m was provided between the basin edge and the beginning of the internal side slopes. This setback ensures safe pedestrian access, facilitates maintenance activities, and prevents accidental slippage into the basin.

The internal side slopes were designed with a gradient of 1:3 (vertical to horizontal), consistent with the maximum slopes recommended for vegetated SuDS basins to ensure stability, ease of maintenance and good vegetation establishment. In addition, a low ornamental garden barrier was placed around the perimeter of the basin to provide a clear visual delineation between the usable green areas and the detention basin, enhancing safety and preventing unintended access.

The total internal depth of the basin was set to 1.20 m, a value that provides the required temporary storage while maintaining safe side slopes and ensuring that the basin remains visually unobtrusive within the landscape. A freeboard of 0.30 m was incorporated above the maximum operational water level, in accordance with SuDS guidance for above-ground storage structures, providing an additional safety margin during extreme events or temporary blockages.

The basin floor consists of two engineered layers. The upper 0.30 m correspond to a topsoil layer that supports vegetation and contributes to water quality improvement by trapping suspended solids. Immediately below, a 0.30 m granular transition layer was installed. This layer serves two functions: (i) it evenly distributes the loads applied at the surface and (ii) it facilitates controlled percolation of water towards the underlying geocellular storage modules. Although permeable internally, this granular layer does not allow infiltration into the surrounding soil, as the geocellular units are fully encapsulated within an impermeable geomembrane, ensuring that the detention system operates exclusively as a controlled-flow storage structure without groundwater interaction.

### **Geocellular tank layout and storage capacity**

This geocellular configuration was applied to both detention basins, each of

which incorporates the same three-layer modular arrangement and the same construction stratigraphy described below.

The subsurface detention volume is provided by modular geocellular units corresponding to the M2014 system supplied by Greening Solution (Figure 3.22). Each module has external dimensions of 0.68 m  $\times$  0.41 m  $\times$  0.45 m (length  $\times$  width  $\times$  height), yielding a gross volume of:

$$V_{\text{mod}} = 0.68 \times 0.41 \times 0.45 \approx 0.125 \text{ m}^3.$$

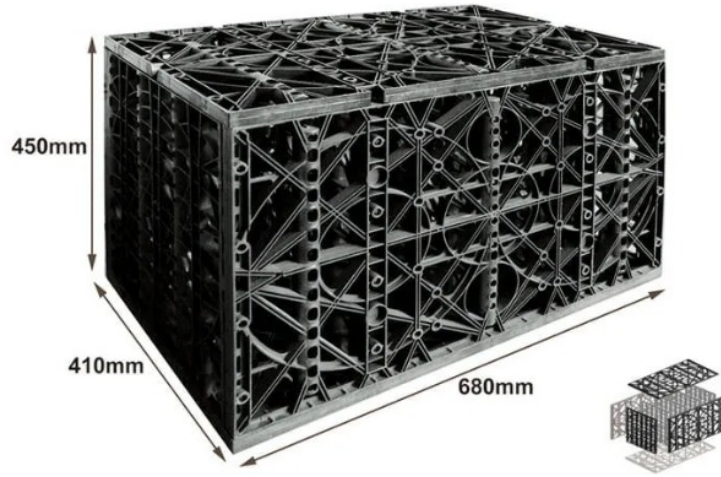


**Figure 3.22:** *Geocellular modular unit selected for the subsurface storage system (dimensions: 680  $\times$  410  $\times$  450 mm). Image source: Greening Solution [32]*

Based on the manufacturer’s specifications, a void ratio of approximately 95 % was adopted, resulting in an effective storage volume per module of:

$$V_{\text{eff}} = 0.95 V_{\text{mod}} \approx 0.119 \text{ m}^3.$$

These units were selected due to their high void ratio, structural strength, and compatibility with buried installations in green areas and light-traffic surfaces. Their modular configuration allows efficient use of the available footprint, simple volumetric scaling, and compatibility with the layered construction adopted in this project, including the granular bedding, lateral surround, and impermeable geomembrane encapsulation [32].

The geocellular tank was arranged within a rectangular footprint of 9 m  $\times$  56 m. In plan view, the modules are placed with their 0.68 m dimension along

the 56 m direction and the 0.41 m dimension along the 9 m direction. This configuration accommodates:

$$n_{56} = \left\lfloor \frac{56}{0.68} \right\rfloor = 82 \quad \text{modules along the 56 m side,}$$

$$n_9 = \left\lfloor \frac{9}{0.41} \right\rfloor = 21 \quad \text{modules along the 9 m side,}$$

resulting in a total of:

$$N_{\text{layer}} = 82 \times 21 = 1722$$

modules per layer.

The effective storage volume provided by one layer of modules is therefore:

$$V_{\text{layer}} = N_{\text{layer}} V_{\text{eff}} = 1722 \times 0.119 \approx 205 \text{ m}^3.$$

To meet the design requirement of 584 m<sup>3</sup>, three stacked layers were adopted, providing a total effective volume of:

$$V_{\text{tot}} = 3 V_{\text{layer}} \approx 614 \text{ m}^3,$$

which satisfies the storage requirement with a modest safety margin. The three superposed layers result in a structural storage height of:

$$H_{\text{store}} = 3 \times 0.45 = 1.35 \text{ m.}$$

This height is incorporated into the vertical stratigraphy of the detention basin system. The geocellular structure is fully enclosed in an impermeable geomembrane, ensuring that the system functions as a controlled-flow detention volume without interaction with the surrounding soil. Figure 3.26 illustrates the main components of the underlying geocellular storage system. From top to bottom, the system integrates the surface detention function with the subsurface modular storage units through a stratified and hydraulically controlled configuration.

**Granular transition layer (washed river sand).** Immediately beneath the topsoil lies a granular transition layer composed of washed river sand without fines. This material provides uniform load distribution and facilitates controlled percolation toward the geocellular modules. In this project, a thickness of 0.15 m was adopted between the detention basin floor and the underlying impermeable polypropylene liner, as recommended for separation, protection and hydraulic uniformity.

**Geocellular storage modules.** The subsurface storage volume is formed by modular geocellular units encased in a protective geotextile. These modules provide high void storage capacity and maintain structural stability under the overlying soil layers. Their vertical and lateral surfaces are wrapped to prevent soil intrusion while allowing internal water movement within the tank.

**Impermeable polypropylene plastic liner.** Surrounding the geocellular modules, a continuous polypropylene geomembrane provides full waterproofing of the storage system. This ensures that no infiltration occurs into the surrounding soil and that all detained water is retained for controlled discharge toward the sewer network.

**Granular bedding layer.** Below the geocellular units, a bedding layer of compacted granular material provides a stable and level foundation for the retention tank and ensures uniform distribution of vertical stresses.

**Pump chamber and access margin.** A dedicated pump chamber is positioned adjacent to the geocellular structure. For operational and maintenance purposes, the pump is located beneath the 1 m access margin left at the edge of the detention basin. This offset ensures safe access for inspection, maintenance and pump replacement without interfering with the functional area of the basin. The pump extracts the detained water from the geocellular system and conveys it to the public stormwater network in compliance with the regulated outflow limit.

A submersible electric pump with a design flow rate of  $Q = 10$  L/s is adopted for each basin. The diameter of the discharge pipe is not specified in this thesis, as it depends on the final pump model selected during detailed design and on manufacturer recommendations regarding allowable velocities and head losses. Nevertheless, for indicative purposes, commercial discharge pipes in the range of DN 75–90 mm typically accommodate flow rates of this magnitude while maintaining acceptable hydraulic performance. The final sizing of the pump and its associated discharge pipe is therefore left to the executive design stage, where the specific pump curve, installation depth, and required operating head can be accurately assessed.

**Overall system integration.** Altogether, the components shown in the figure demonstrate the layered configuration that enables the surface detention basin to function in tandem with the subsurface geocellular tank, ensuring temporary storage, structural safety, protected infiltration pathways within the tank, and controlled discharge to the sewer network.

### **Effect of Shallow Groundwater Levels on the Applicability of the Proposed Solution**

Although three of the selected cities (Cagliari, Palermo, and Genova) exhibit a shallow groundwater table, as reported in Table 2.8, this condition does not compromise the applicability of the proposed stormwater management system. According to [1], infiltration cannot be considered when the phreatic level lies close to the ground surface or when insufficient geotechnical information is available. For this reason, and to ensure methodological consistency across all cities, infiltration was excluded from the hydrological analysis.

The adopted SuDS configuration consists of a fully sealed subsurface detention tank formed by modular geocellular units completely wrapped in an impermeable geomembrane. As described in Section 3.2.2, this encapsulation prevents any hydraulic interaction between the stored water and the surrounding soil, ensuring that the system operates exclusively as a detention volume with controlled discharge to the sewer network.

Consequently, the presence of a shallow water table affects only the external hydrostatic conditions acting on the structure, which can be addressed through appropriate structural design of the geocellular tank. The hydraulic behaviour of the system, including the storage process and the regulated outflow, remains unchanged. Therefore, the same detention solution can be consistently applied in all analysed cities, regardless of groundwater depth.

## **3.3 Design Drawings**

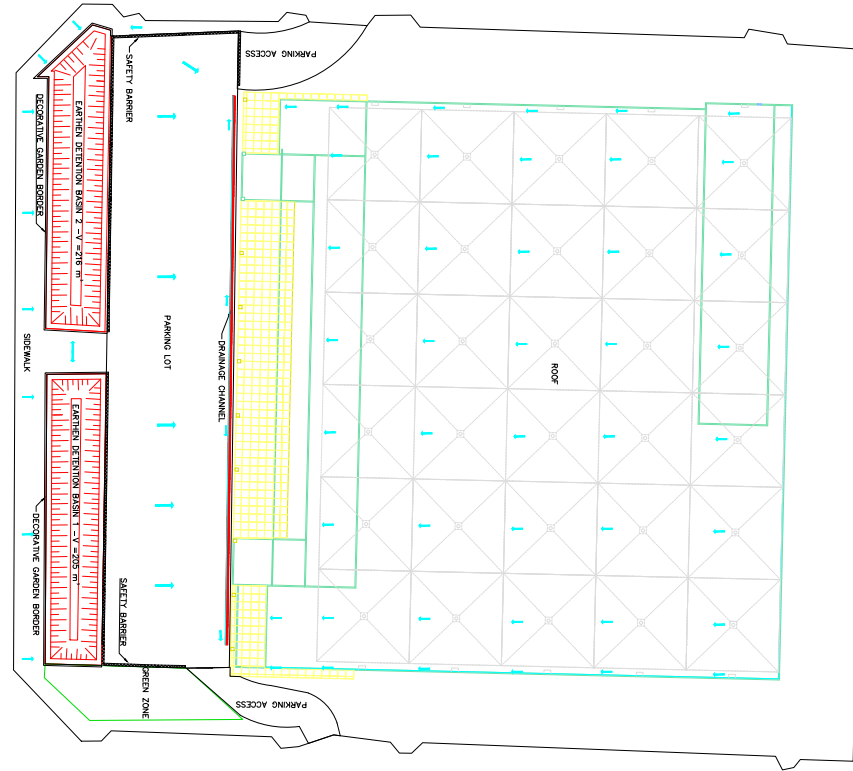


**Figure 3.23:** General plan view of the study area, showing the layout of the surface drainage elements, the location of the detention basins and subsurface tanks, and the direction of stormwater flow across the site. Scale 1:1000



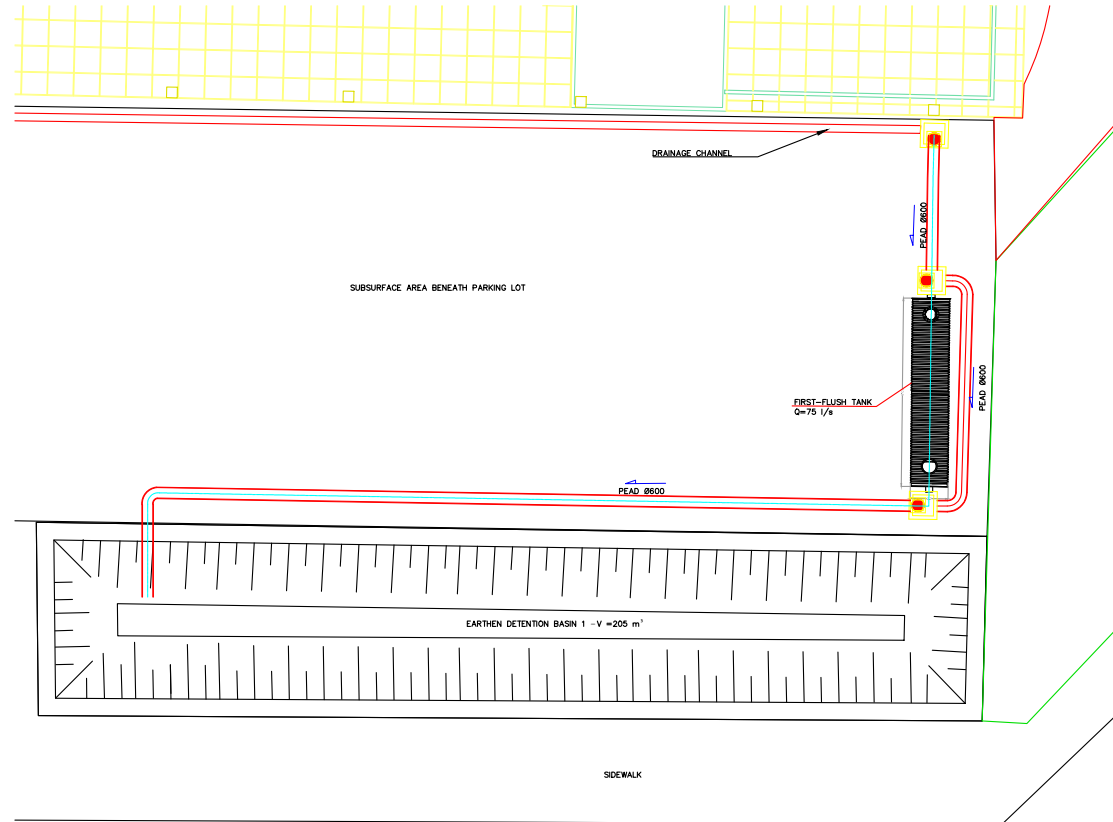


**Figure 3.24:** Plan view of the *FIRST-FLUSH TANK* and *Detention Basin 1*. Scale 1:250 [33].

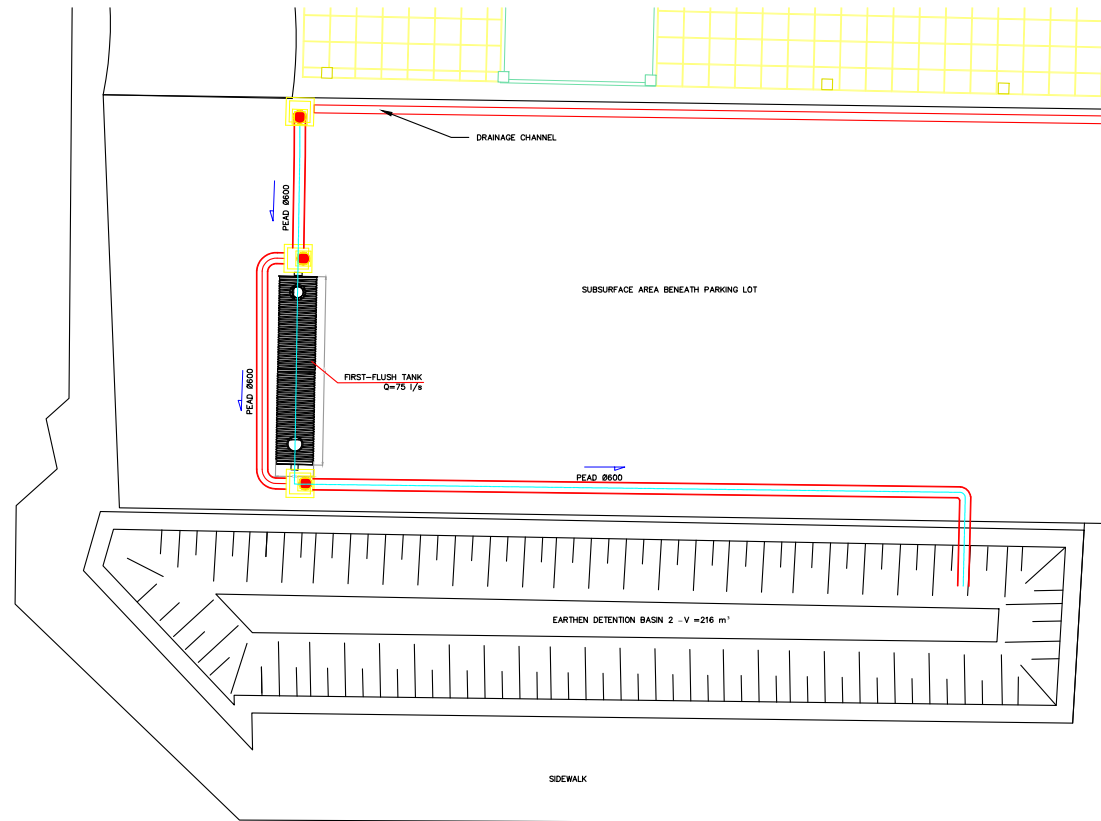


**Figure 3.25:** Plan view of the FIRST-FLUSH TANK and Detention Basin 2. Scale 1:250 [33].

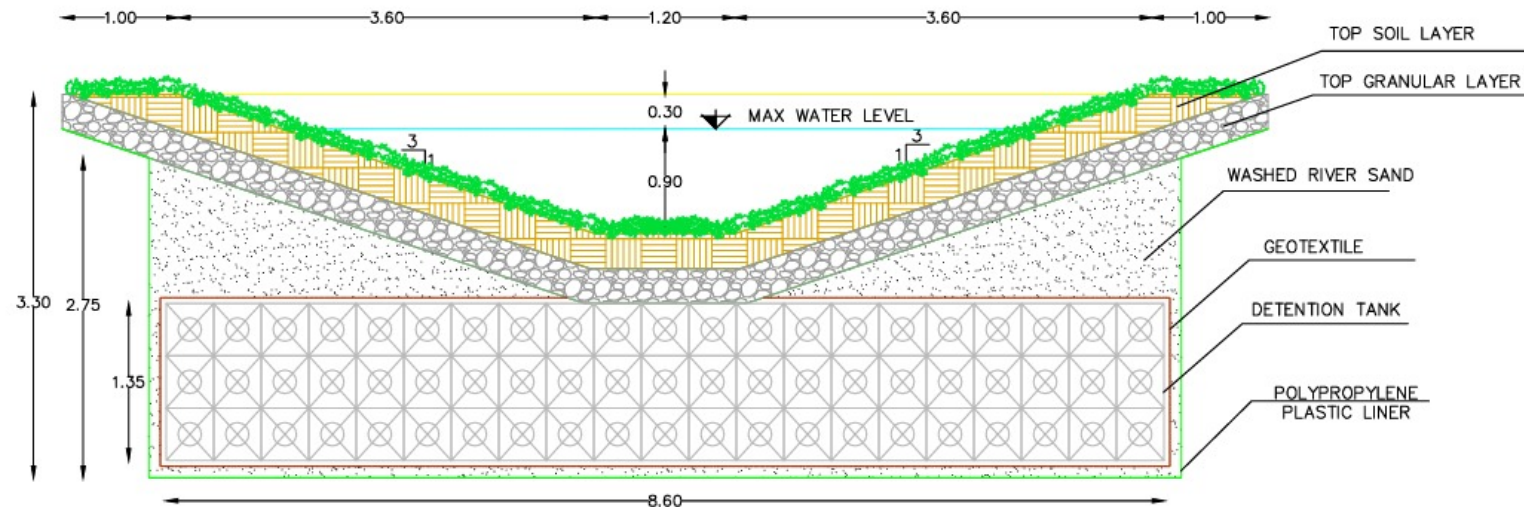


**Figure 3.26:** Section view of the detention basin 1 and subsurface tank, showing the surface basin geometry, the stratigraphy of the soil and granular layers, and the connection to the underlying geocellular storage system scale 1:50[33].

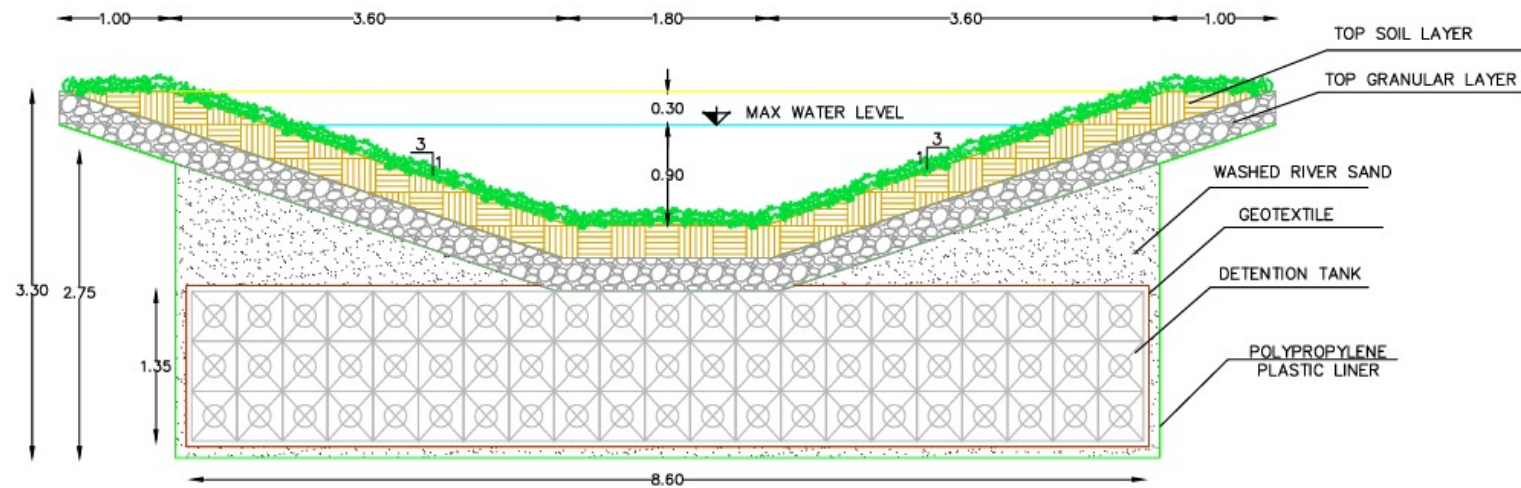


**Figure 3.27:** Section view of the detention basin 2 and subsurface tank, showing the surface basin geometry, the stratigraphy of the soil and granular layers, and the connection to the underlying geocellular storage system. scale 1:50 [33].

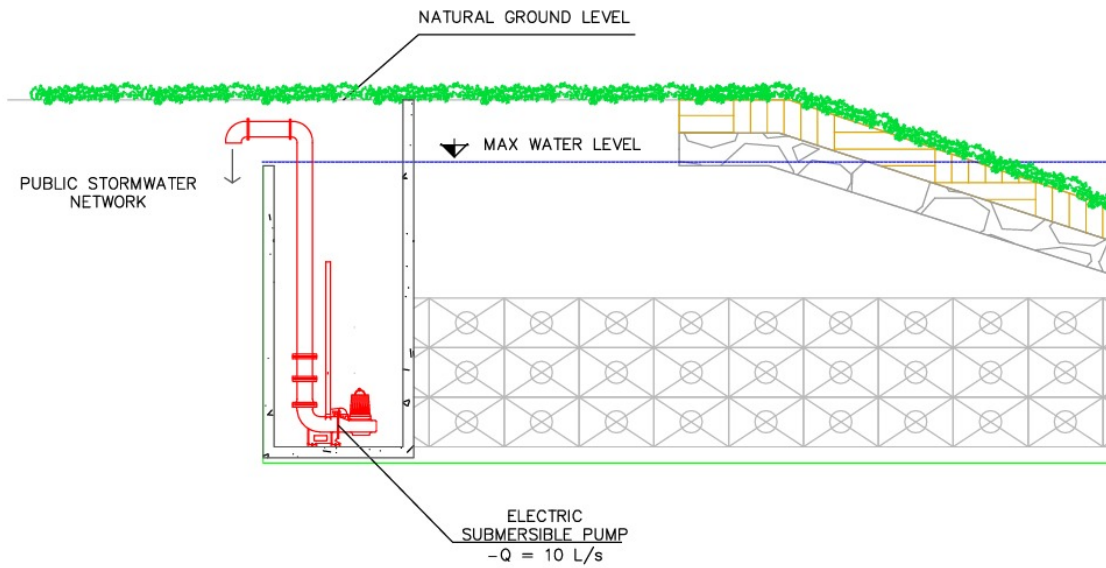


**Figure 3.28:** Longitudinal section of the detention basin and subsurface tank, showing the natural ground level (NGL), the geocellular storage system, and the technical compartment housing the submersible electric pump ( $Q = 10 \text{ L/s}$ ) and its discharge connection to the public stormwater network. scale 1:50



**Figure 3.29:** *3D model of the proposed stormwater detention system – View 1 - Close-up view [34]*





**Figure 3.30:** *3D model of the proposed stormwater detention system – View 2 - Detention basin displayed in its dry (empty) condition [34]*

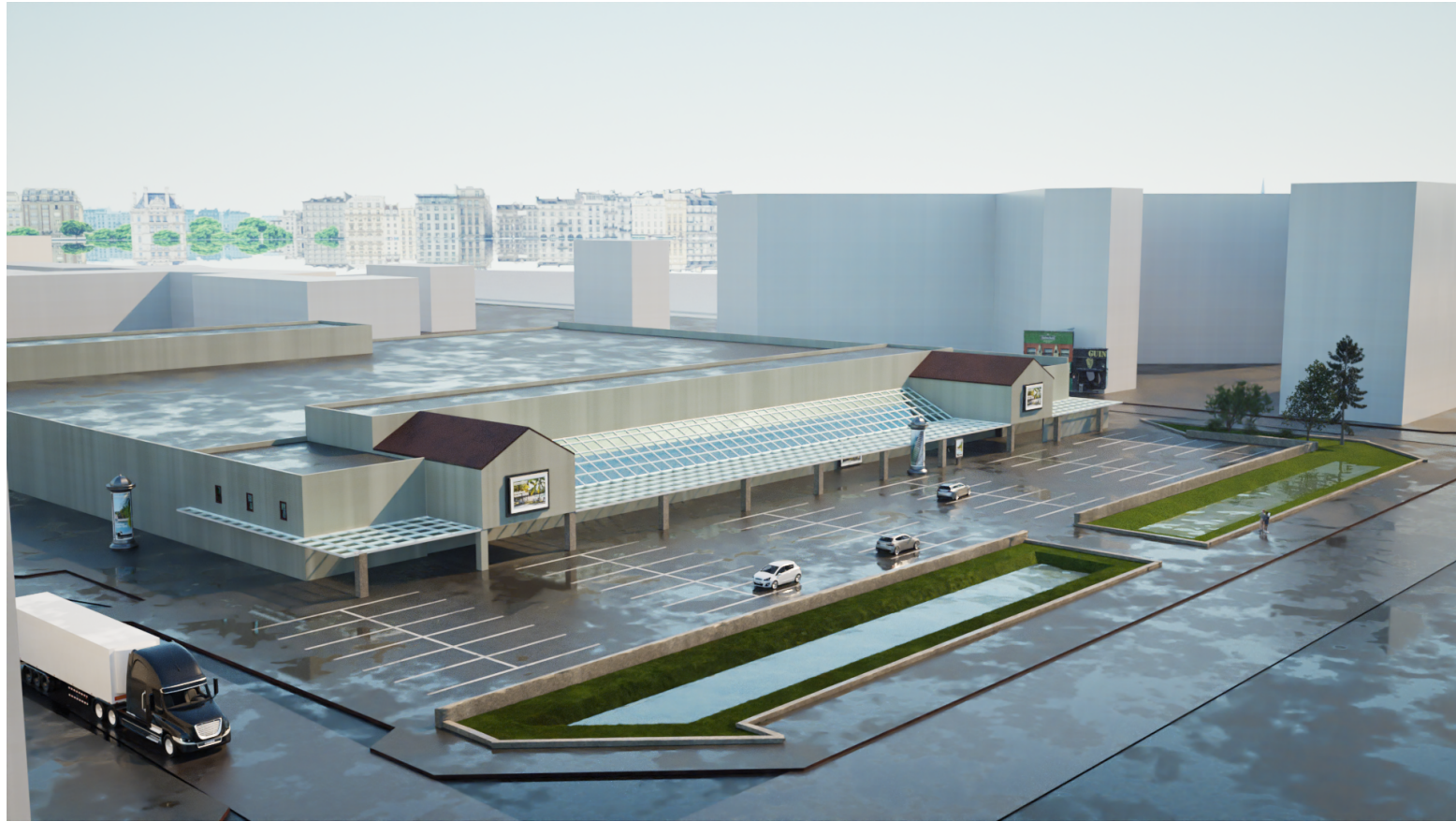


**Figure 3.31:** *3D model of the proposed stormwater detention system – View 3 - Detention basin shown at its maximum water level [34]*



## 3.4 Discussion of Results

The results obtained in this study clearly show that the application of the *metodo dettagliato* prescribed by [1] leads systematically to a detention volume governed by the minimum regulatory requirement, regardless of the local climatic conditions considered. Although the six selected cities exhibit substantial differences in rainfall intensity, design hyetographs, and peak inflow discharges (see Tables and Figures of Chapter 3), these differences do not translate into the final design volume.

The fundamental reason is that, for every city, the hydrologically derived detention volume  $V_{\text{det}}$  is significantly lower than the minimum normative volume  $V_{\text{min}}$ , which for the considered project area equals  $1588.7 \text{ m}^3$  (see Table 3.3). As a consequence, the design volume  $V_{\text{proj}}$  coincides with  $V_{\text{min}}$  in all cases.

### 3.4.1 Comparison Between Hydrological Volumes and the Normative Minimum

The calculated  $V_{\text{det}}$  values demonstrate a wide climatic spread (see Table 3.3):

- Aosta shows the smallest detention volume requirement ( $245.1 \text{ m}^3$ ), which is approximately 84.6% lower than the normative threshold, corresponding to an overestimation factor of about 6.5.
- Cagliari and Palermo require  $697.3\text{--}744.7 \text{ m}^3$ , i.e. 56–60% less than  $V_{\text{min}}$ .
- Torino and Roma, despite having higher rainfall intensities, still require only  $892.3\text{--}1039.5 \text{ m}^3$ , corresponding to a 35–44% reduction relative to the regulatory minimum.
- Genova, the city with the most intense rainfall regime and the highest peak inflow ( $5.1 \text{ m}^3/\text{s}$ ), produces the largest hydrological volume ( $1443.6 \text{ m}^3$ ). Even in this extreme case,  $V_{\text{det}}$  remains about 9% below the normative minimum.

This last point is particularly meaningful: even under the most intense climatic conditions among the study locations, the hydrological volume does not exceed the minimum regulatory requirement. Thus, the regulation remains the dominant factor in determining the design volume, independently of city-specific rainfall characteristics.

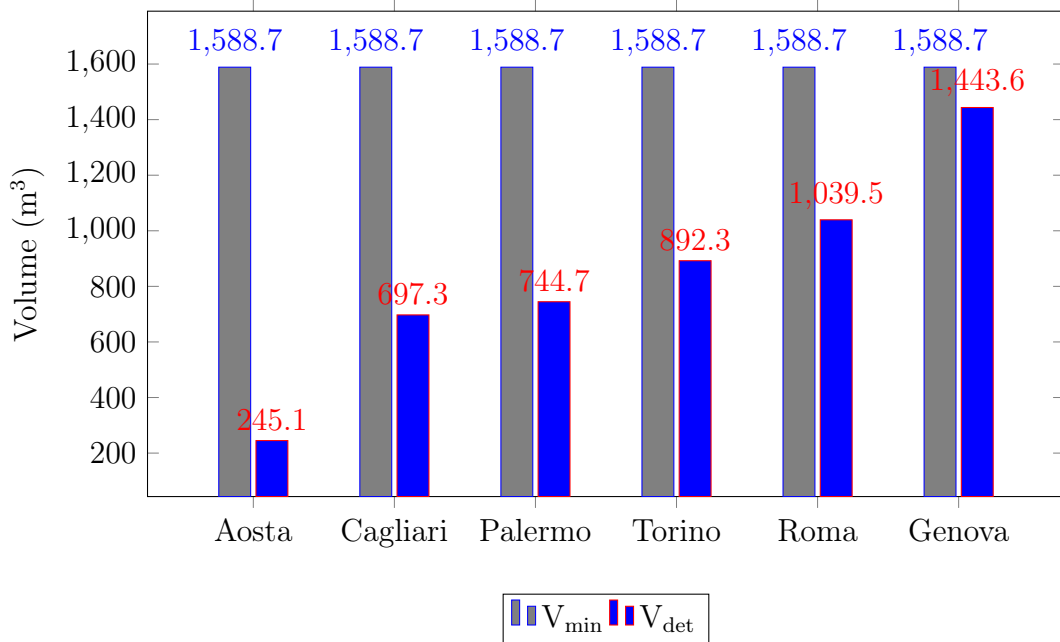


**Figure 3.32:** Comparison between minimum required volume ( $V_{min}$ ) and design detention volume ( $V_{det}$ ) for the six cities.

### 3.4.2 Overall Interpretation

In summary, although the hydrological analysis reveals significant climatic variability among the selected cities, with peak intensities differing by a factor of up to eight and peak inflow discharges varying by more than an order of magnitude, this variability does not influence the final design. Under the Lombardy regulation, the minimum volume criterion fully dominates the outcome, overshadowing the climatic differences highlighted in previous sections. As a result, the variability in design rainfall and runoff conditions is not reflected in the detention system sizing.

# Conclusions

This thesis examined how a single commercial development behaves hydrologically when applied to different Italian climatic contexts under one uniform regulatory framework. The analysis compared the detention volumes obtained for six cities using the detailed procedure prescribed by the Lombardy Regional Regulation (R.R. 19 April 2019, n. 8), while keeping all methodological assumptions strictly constant.

The results show that the hydrologically derived detention volumes vary significantly across the selected locations, reflecting the climatic diversity of Italy. Cities with lower rainfall intensities, such as Aosta, produce markedly smaller values of detention volumes, whereas cities with more intense precipitation regimes, such as Genova or Roma, generate higher inflow peaks and larger associated storage requirements. However, despite this variability, all computed values of detention volumes remain below the minimum storage requirement established by the regulation for highly critical areas. As a consequence, the final design volume is the same for every city, equal to  $V_{\text{proj}} = V_{\text{min}} = 1588.7 \text{ m}^3$ .

This outcome provides a clear answer to the central research question. When the Lombardy Regulation is applied uniformly across different climatic contexts, the minimum normative threshold dominates the design process, resulting in a uniform storage volume regardless of local rainfall characteristics. The comparison therefore illustrates that, under the regulatory constraints of Area A, climatic variability does not translate into differentiated detention sizing. Instead, the regulation ensures a robust and highly conservative margin of safety across all tested scenarios.

Beyond the quantitative findings, the thesis also explored a feasible stormwater management configuration capable of satisfying the regulatory requirements in all six cities. The proposed solution—based on subsurface geocellular storage combined with surface detention—demonstrates that a single design approach can be consistently applied even in locations with shallow groundwater levels, provided that infiltration is excluded and the system is fully sealed.

The study's main contribution lies in demonstrating the implications of applying a region-specific regulation to geographically diverse contexts while preserving full methodological uniformity. This provides insight into the balance between climatic variability and normative constraints, and highlights how prescriptive minimum values can govern design outcomes in multi-city comparative assessments.

Some limitations must be acknowledged. The exclusion of infiltration, required by the lack of site-specific hydrogeological data, restricts the anal-

ysis to detention-only solutions. In addition, the study focuses on a single urban typology, which limits the generalisation of results to other types of developments. The application of only one regulatory framework also means that the findings reflect a specific normative perspective.

Future work could extend this analysis by incorporating detailed soil investigations, evaluating alternative design rainfall methodologies, or comparing multiple regional regulations within the same multi-city framework. Further studies could also investigate how flexible or adaptive regulatory criteria might better reflect local climatic conditions while maintaining hydraulic safety.

Overall, this thesis demonstrates that, when a strict and uniform regulatory framework is applied, climatic variability alone does not lead to differentiated detention volumes. Instead, the minimum normative requirement determines the final design in all cases, offering both robustness and a clear understanding of the regulatory implications for stormwater management across different regions of Italy.

# References

- [1] Regione Lombardia, *Regolamento regionale 19 aprile 2019, n. 8 - criteri e metodi per il rispetto del principio dell'invarianza idraulica e idrologica*, Bollettino Ufficiale della Regione Lombardia, Serie Ordinaria n. 17 del 23 aprile 2019, 2019.
- [2] R. Govindaraju and A. Goyal, "Rainfall and infiltration," in *Rainfall: Modeling, Measurement and Applications*, R. Morbidelli, Ed., Elsevier, 2022, pp. 367–390. DOI: 10.1016/B978-0-12-822544-8.00007-X.
- [3] R. Morbidelli, C. Saltalippi, A. Flammmini, and C. Corradini, "Rainfall and development of floods," in *Rainfall: Modeling, Measurement and Applications*, R. Morbidelli, Ed., Elsevier, 2022, pp. 335–366. DOI: 10.1016/B978-0-12-822544-8.00006-8.
- [4] V. Novotny, *Urban and Highway Stormwater Pollution: Concepts and Engineering*. John Wiley & Sons, 2010, ISBN: 9780470476086.
- [5] J. R. M. Hosking and J. R. Wallis, *Regional Frequency Analysis: An Approach Based on L-Moments*. Cambridge, UK: Cambridge University Press, 1997.
- [6] S. Grimaldi, A. Petroselli, F. Serinaldi, and L. V. Noto, "Design rainfall estimation in the upper tiber river basin by l-moments and regional frequency analysis," *Hydrology and Earth System Sciences*, vol. 15, no. 2, pp. 449–470, 2011. DOI: 10.5194/hess-15-449-2011.
- [7] S. C. Service, *Hydrology: National Engineering Handbook, Section 4*. Washington, D.C.: U.S. Department of Agriculture, 1956.
- [8] M. Pinna, *Italy köppen climate classification according to pinna*, Wikimedia Commons, Licencia CC BY-SA 3.0, 2017. [Online]. Available: [https://it.wikipedia.org/wiki/File:Italy\\_K%C3%B6ppen\\_climate\\_classification\\_according\\_to\\_Pinna.png](https://it.wikipedia.org/wiki/File:Italy_K%C3%B6ppen_climate_classification_according_to_Pinna.png).
- [9] ARPA Sicilia, *Arpa sicilia - agenzia regionale per la protezione ambientale*, <https://www.arpa.sicilia.it>, Accessed 2025, 2025.
- [10] SIR Toscana, *Sir toscana - servizio idrologico regionale*, <https://www.sir.toscana.it>, Accessed 2025, 2025.
- [11] ARPA Lazio, *Arpa lazio - agenzia regionale per la protezione ambientale*, <https://www.arpalazio.gov.it>, Accessed 2025, 2025.
- [12] ARPAB Basilicata, *Arpab basilicata - agenzia regionale per la protezione dell'ambiente della basilicata*, <https://www.arpab.it>, Accessed 2025, 2025.

- [13] ARPACAL Calabria, *Arpacal calabria - agenzia regionale per la protezione dell'ambiente della calabria*, <https://www.arpacalabria.gov.it>, Accessed 2025, 2025.
- [14] ARPA Piemonte, *Arpa piemonte - agenzia regionale per la protezione ambientale*, <https://www.arpa.piemonte.it>, Accessed 2025, 2025.
- [15] ARPA Marche, *Arpa marche - agenzia regionale per la protezione ambientale*, <https://www.arpa.marche.it>, Accessed 2025, 2025.
- [16] Meteotrentino, *Meteotrentino - servizio meteorologico della provincia autonoma di trento*, <https://www.meteotrentino.it>, Accessed 2025, 2025.
- [17] P. Claps, G. Evangelista, D. Ganora, P. Mazzoglio, and I. Monforte, *Foca: Italian flood and catchment atlas*, Zenodo, 2023. DOI: 10.5281/zenodo.10446258. [Online]. Available: <https://doi.org/10.5281/zenodo.10446258>.
- [18] ARPA Valle d'Aosta, *Qualità delle acque sotterranee della regione valle d'aosta – report 2023*, Monitoraggio quantitativo e piezometrico, 2023.
- [19] Servizio Geologico d'Italia and Regione Autonoma della Sardegna, *Foglio 557 – cagliari. carta geologica d'italia 1:50.000, progetto carg*, Informazioni idrogeologiche sulla soggiacenza urbana (2–10 m), 2001.
- [20] Città Metropolitana di Palermo, *Relazione geologica e indagini – plesso scolastico regina margherita, via casa professa 3*, Documento tecnico con rilevazioni piezometriche. Superficie piezometrica a –5.25 m dal piano campagna, 2022.
- [21] ARPA Piemonte, *Rete di monitoraggio piezometrica – stazione 00127210001*, Piezometric monitoring network, 2025. [Online]. Available: [https://webgis.arpa.piemonte.it/monitoraggio\\_qualita\\_acque/indexpiez.php?numcodice=00127210001](https://webgis.arpa.piemonte.it/monitoraggio_qualita_acque/indexpiez.php?numcodice=00127210001).
- [22] Città Metropolitana di Roma Capitale, *Carta idrogeologica – sistema informativo territoriale*, Hydrogeological map and groundwater information, 2025. [Online]. Available: <https://g3w-suite.cittametropolitanaroma.it/it/map/carta-idrogeologica/>.
- [23] Comune di Genova, *Relazione geologica e studio delle falde – area ikea genova campi*, Documento tecnico utilizzato per la valutazione della soggiacenza nell'area urbana di Genova, 2011.
- [24] Google Earth Pro, *Google earth pro, version 7.3.6*, Google LLC, Accessed: Aug. 18, 2025, 2025.

- [25] Roofcorp. “The ultimate guide to commercial flat roofing.” Accessed: Aug. 17, 2025. (2025).
- [26] Plaincode, *Clinometer + bubble level, mobile application*, Mobile app, Android/iOS, Accessed: Aug. 18, 2025, 2025.
- [27] HIDROSTANK, *Drenaje urbano suds – sistemas modulares geocelulares*, Accessed: 2025-02-15, 2024. [Online]. Available: <https://www.hidrostantk.com/hidrostantk/es/portfolio/drenaje-urbano-suds/>.
- [28] CIRIA, *The SuDS Manual (CIRIA C753)*. London, UK: Construction Industry Research and Information Association, 2015.
- [29] Repubblica Italiana, *Decreto legislativo 3 aprile 2006, n. 152 – norme in materia ambientale*, Testo Unico Ambientale, 2006. [Online]. Available: <https://www.normattiva.it>.
- [30] Regione Lombardia, *D.g.r. 7/18532/2004 – criteri tecnici per il trattamento delle acque di prima pioggia e di lavaggio strade*, 2004. [Online]. Available: <https://www.regione.lombardia.it>.
- [31] Regione Piemonte, *D.g.r. piemonte 14 febbraio 2012, n. 46-11968 – linee guida per la gestione delle acque meteoriche di dilavamento*, 2012. [Online]. Available: <https://www.regione.piemonte.it>.
- [32] Greening Solution, *Modular geocellular units – underground water tank system*, Accessed: 2025-02-20, 2024. [Online]. Available: <https://es.greening-solution.com/underground-water-tank/modular-geocellular-units/>.
- [33] Autodesk, Inc., *Autodesk civil 3d*, Computer Software, 2024. [Online]. Available: <https://www.autodesk.com/products/civil-3d/overview>.
- [34] Autodesk, Inc., *Autodesk revit*, Computer Software, 2024. [Online]. Available: <https://www.autodesk.com/products/revit/overview>.